**Advances in Bioresearch**
Adv. Biores., Vol 17 (4) April 2026: 170-197
©2026 Society of Education, India
Print ISSN 0976-4585; Online ISSN 2277-1573
Journal's URL:http://www.soeagra.com/abr.html
CODEN: ABRDC3
DOI: 10.15515/abr.0976-4585.17.4.170197

Advances in Bioresearch

## ORIGINAL ARTICLE

# Exploration of Bioactive Constituents of *Feronia elephantum* Through Phytochemical Evaluation, GC–MS Analysis, and Computational Approaches

**Inzamamul Haq Ameer Shaikh[1]*, Sharad D. Tayade[2]**, Arfin S. Tamboli[1], Kedar Kailas Ganjare[1], Vijay S. Borkar[3], Jyoti Bhushan Khedekar[4]**

[*1] Research Scholar, Department of Industrial Pharmacy, Shri Sant Gajanan Maharaj College of Pharmacy, Buldana-443001, Maharashtra, India

[**2] Department of Industrial Pharmacy, Shri Sant Gajanan Maharaj College of Pharmacy, Buldana-443001, Maharashtra, India

[3] Department of Pharmaceutical Chemistry, Shri Sant Gajanan Maharaj College of Pharmacy, Buldana-443001, Maharashtra, India

[4] Department of Pharmaceutics, Shri Sant Gajanan Maharaj College of Pharmacy, Buldana-443001, Maharashtra, India

***Correspondence author email:** shaikhinzi7996@gmail.com; sharad_tayade1@rediffmail.com

**ABSTRACT**

*The present study aimed to investigate the phytochemical profile, safety, and therapeutic potential of Feronia elephantum through integrated experimental and computational approaches. Hydroalcoholic extraction using the Soxhlet method yielded 9.67% extract, indicating efficient recovery of bioactive constituents. Organoleptic and physicochemical evaluation confirmed good quality, with slightly acidic pH, low moisture content, and absence of contaminants such as heavy metals and pesticide residues. Preliminary phytochemical screening revealed the presence of diverse constituents, including fats and oils, phenolics, flavonoids, tannins, steroids, alkaloids, and glycosides, suggesting significant pharmacological potential. Microbial analysis confirmed the absence of pathogenic microorganisms, indicating microbiological safety of the extract. GC–MS analysis identified a wide range of compounds, including phenolics, fatty acids, sterols, and triterpenoids, with cyclolanostane derivatives as major constituents. Molecular docking studies against the COX-2 enzyme (PDB ID: 5KIR) demonstrated strong binding affinities for several compounds, particularly FE-09 (−8.7 kcal/mol), FE-10 (−8.5 kcal/mol), FE-13 (−8.1 kcal/mol), and FE-15 (−8.1 kcal/mol), comparable to the reference drug Rofecoxib. These interactions were supported by hydrogen bonding and hydrophobic interactions within the active site. ADMET and drug-likeness analysis revealed that FE-15, along with FE-02 and FE-04, exhibited favorable pharmacokinetic and safety profiles, including balanced absorption, distribution, metabolism, and low toxicity risks. Overall, the study highlights Feronia elephantum as a promising source of bioactive compounds with potential anti-inflammatory activity and supports its further development as a therapeutic agent.*

**KEYWORDS:** *Feronia elephantum*, Phytochemical screening, GC–MS analysis, Molecular docking, COX-2 inhibition, ADMET analysis

Received 24.02.2026 Revised 30.03.2026 Accepted 21.04.2026

**How to cite this article:**
Inzamamul Haq Ameer S, Sharad D. T, Arfin S. T, Kedar Kailas G, Vijay S. B, Jyoti B K. Exploration of Bioactive Constituents of *Feronia elephantum* Through Phytochemical Evaluation, GC–MS Analysis, and Computational Approaches . Adv. Biores. Vol 17 [4] April 2026. 170-197

## INTRODUCTION

Medicinal plants have long served as a cornerstone in the discovery of therapeutic agents, offering a vast reservoir of bioactive compounds with diverse pharmacological activities. In recent years, there has been a growing interest in exploring plant-derived natural products as safer and more effective alternatives to synthetic drugs, particularly for the management of inflammatory disorders [1–3]. Chronic inflammation is associated with several pathological conditions, including arthritis, cardiovascular diseases, and metabolic syndromes, necessitating the development of novel anti-inflammatory agents with improved

safety profiles. Among the various molecular targets, cyclooxygenase-2 (COX-2) plays a crucial role in mediating inflammatory responses, making it a promising target for drug discovery [4–6].
*Feronia elephantum*, commonly known as wood apple, is a medicinal plant widely distributed in tropical regions and traditionally used in Ayurveda and folk medicine for treating various ailments such as digestive disorders, inflammation, and infections. Different parts of the plant, including leaves, bark, and fruit, are known to possess significant therapeutic properties attributed to the presence of diverse phytoconstituents such as flavonoids, tannins, phenolics, alkaloids, and glycosides. These compounds are recognized for their antioxidant, anti-inflammatory, antimicrobial, and hepatoprotective activities [7–9]. Despite its traditional significance, systematic scientific evaluation of its phytochemical composition and molecular mechanisms remains limited.
Phytochemical screening serves as a fundamental step in identifying the classes of bioactive compounds present in plant extracts. It provides essential insights into the chemical nature of constituents that may contribute to therapeutic efficacy. Complementing this, Gas Chromatography–Mass Spectrometry (GC–MS) analysis offers a powerful analytical tool for the identification and characterization of volatile and semi-volatile compounds within complex plant matrices This technique enables the detection of a wide range of compounds, including fatty acids, sterols, and phenolic derivatives, thereby providing a detailed chemical fingerprint of the extract [10–12].
In addition to experimental techniques, computational approaches have emerged as valuable tools in modern drug discovery. Molecular docking studies allow for the prediction of binding affinity and interaction patterns between bioactive compounds and target proteins, thereby facilitating the identification of potential drug candidates. Furthermore, in silico ADMET (Absorption, Distribution, Metabolism, Excretion, and Toxicity) analysis provides critical information on pharmacokinetic behavior and safety profiles, helping to prioritize compounds with favorable drug-like properties. These integrated approaches significantly enhance the efficiency and accuracy of the drug discovery process [13,14].
Therefore, the present study aims to explore the bioactive constituents of *Feronia elephantum* through a comprehensive approach involving phytochemical evaluation, GC–MS analysis, and computational studies. The study focuses on identifying key phytoconstituents, evaluating their interaction with the COX-2 enzyme, and assessing their pharmacokinetic and toxicity profiles. This integrated investigation not only provides scientific validation for the traditional use of *Feronia elephantum* but also highlights its potential as a promising source of novel anti-inflammatory agents for future drug development.

## MATERIAL AND METHODS

### Collection of Plant Material and Authentication

Feronia elephantum herb was collected in December 2025 from a local area of Buldhana, Maharashtra, India. The collected plant material was used to prepare a herbarium specimen and authenticated by the Department of Botany, Government Degree College, Kukatpally, Medchal District, Telangana (affiliated to Osmania University). The authentication was carried out by P. Suresh Babu, Assistant Professor of Botany. A voucher specimen (No. 0409) was deposited for future reference. The authentication certificate was issued on 04.03.2026. Following authentication, the plant material was subjected to extraction. The images of the plant are presented in Figure 1.

Figure 1: The *Feronia elephantum* plant

### Soxhlet Extraction using Hydroalcoholic Solvent

For extraction, *Feronia elephantum* leaves and bark were collected and washed with distilled water to remove dust and foreign particles, followed by shade drying at room temperature for one week. Drying under ambient conditions is essential to prevent the loss of volatile phytoconstituents. Approximately 500 g of the dried plant material was then ground into a coarse powder for further processing. The

powdered material was subjected to Soxhlet extraction using a hydroalcoholic solvent (ethanol:water mixture) in a Soxhlet apparatus. The extraction was continued until complete exhaustion of phytoconstituents from the plant material. The gradual change to a dark-colored solvent in the round-bottom flask (RBF), along with the fading colour of the plant matrix in the extraction chamber, indicated efficient extraction of constituents. The process was carried out for approximately 24 hours, allowing multiple siphon cycles to ensure maximum recovery of bioactive compounds. After completion, the extract collected in the RBF was transferred into petri dishes, and the solvent was allowed to evaporate naturally at room temperature [15,16]. The resulting concentrated extract was then stored and further subjected to qualitative phytochemical analysis. The working photographs of Soxhlet extraction are depicted in Figure 2.

Figure 2: The Soxhlet extraction of *Feronia elephantum*

**Physicochemical Analysis**

Physicochemical analysis of the extracts was performed using standard methods to evaluate their quality and purity. Colour was observed under natural light, while odour and taste were assessed organoleptically. The pH of 1% and 10% solutions was measured using a calibrated digital pH meter. Foreign matter was determined by separating and weighing extraneous materials from a known quantity of sample, and the percentage was calculated. Loss on drying (LOD) was evaluated by drying the sample at 105°C until a constant weight was obtained. Ash values, including total ash, acid-insoluble ash,

sulphated ash, and water-soluble ash, were determined by incineration and standard treatment procedures to assess inorganic content. Extractive values were determined by macerating the powdered drug in alcohol and chloroform water, followed by filtration and evaporation to calculate alcohol- and water-soluble extractives. Heavy metals (As, Cd, Pb, Hg, Zn, Cu, Cr, Mn) were analyzed using atomic absorption spectroscopy after acid digestion of the samples. Pesticide residues were determined using gas chromatography with an electron capture detector after sample cleanup and concentration, with detection limits in the ppb range [17] .

**Preliminary Phytochemical Screening**

Preliminary phytochemical screening of the crude extract was carried out using standard qualitative tests to identify the presence of various classes of phytoconstituents. Tests for carbohydrates were performed using Molisch's test, while reducing sugars were identified by Fehling's and Benedict's tests, and monosaccharides by Barfoed's test. Proteins were detected using Biuret, Millon's, and Xanthoprotein tests, along with sulphur-containing protein and precipitation tests. Amino acids were confirmed by Ninhydrin, tyrosine, tryptophan, and cysteine tests. Fats and oils were evaluated using solubility and saponification tests. Steroids were identified by Salkowski, Liebermann–Burchard, and Liebermann reactions. Cardiac glycosides were detected using Keller–Killiani and Legal's tests, while anthraquinone glycosides were confirmed by Borntrager's and modified Borntrager's tests. Saponins were identified using the foam test, and cyanogenetic glycosides were evaluated using sodium picrate paper. Flavonoids were detected using Shinoda, lead acetate, ferric chloride, and alkali tests. Alkaloids were identified using Dragendorff's, Mayer's, Wagner's, and Hager's reagents after acid extraction. Tannins and phenolic compounds were confirmed using ferric chloride, lead acetate, iodine, nitric acid, potassium permanganate, gelatin, bromine, and acetic acid tests. The presence or absence of phytoconstituents was determined based on characteristic colour changes or precipitate formation [18–20].

**Microbial Content Determination**

Microbial content of the samples was determined using standard plate count and selective culture methods. For solid samples, 1 g of powder was dispersed in 9 mL of sterile distilled water, while liquid samples (1 mL) were diluted similarly. Serial dilutions were prepared, and microbial load was assessed using the pour plate method. Plates were incubated at 37°C for 24 h, and colony-forming units (CFU) were counted using a colony counter. Results were expressed as the mean of duplicate determinations. Nutrient agar, Cetrimide agar, Salt agar, and MacConkey agar were used for bacterial enumeration, while Sabouraud dextrose agar was used for fungal detection with incubation at 27°C for 72 h. Detection of specific microorganisms was performed using enrichment and selective media techniques. For Escherichia coli, samples were enriched in nutrient broth at 37°C for 24 h, followed by incubation in MacConkey broth at 36–38°C for 48 h; acid and gas production indicated a positive result. For Salmonella spp., enriched cultures were transferred to Selenite and Tetrathionate broths, incubated, and plated on Deoxycholate citrate agar, followed by incubation at 36–38°C for 24 h to observe characteristic colonies. For Shigella spp., enrichment was carried out in alkaline nutrient broth, followed by streaking on Salmonella–Shigella agar and incubation at 37°C for 48 h; non-lactose fermenting colonies were confirmed by biochemical tests such as TSI agar. Detection of Pseudomonas aeruginosa involved enrichment in soyabean–casein digest medium, followed by cultivation on cetrimide agar and confirmation by oxidase test. For Staphylococcus aureus, samples were enriched in peptone water, streaked on Mannitol Salt Agar, and incubated at 37°C for 24 h. Characteristic colonies were confirmed using catalase and coagulase tests [21,22].

**GC–MS Analysis**

Gas Chromatography–Mass Spectrometry (GC–MS) analysis of *Feronia elephantum* extract was performed using a GC–MS system equipped with an electron ionization (EI) source. The sample was introduced in split mode with an injection volume of 1.0 µL. The chromatographic separation was carried out using a suitable capillary column under programmed temperature conditions. The oven temperature was initially maintained at a lower temperature and gradually increased in a programmed manner to ensure proper separation of volatile and semi-volatile compounds across the chromatographic run. The total run time was approximately 58 minutes. Helium was used as the carrier gas at a constant flow rate. The mass spectrometer was operated in electron ionization (EI) mode, and data acquisition was carried out over an appropriate mass range to detect a wide spectrum of compounds. The ion source and interface temperatures were maintained under optimized conditions to ensure efficient ionization and transfer of analytes. The chromatographic and spectral data were recorded and processed using the instrument software. Identification of compounds was performed by comparing the obtained mass spectra with standard reference spectra available in the NIST library database [23].

**Molecular Docking**

Molecular docking analysis was carried out to evaluate the binding affinity and interaction pattern of the selected ligands with the target protein. The three-dimensional (3D) structure of the target protein was retrieved from the Protein Data Bank (PDB) using the PDB ID: 5KIR. The protein structure was prepared using Discovery Studio, where water molecules, co-crystallized ligands, and other heteroatoms were removed, followed by the addition of hydrogen atoms and energy minimization to stabilize the structure. The chemical structures of the selected ligands were obtained from PubChem in SDF format and further optimized using ChemDraw. The ligands were then converted into appropriate file formats (PDB) and subjected to energy minimization prior to docking [24–26]. Docking simulations were performed using PyRx software, which employs the AutoDock Vina algorithm. The prepared protein and ligands were imported into PyRx, and a grid box was defined around the active site of the protein using the coordinates X = 38.556836, Y = 7.633205, Z = 44.477027 to ensure proper coverage of the binding pocket. Default parameters were used for docking, and multiple conformations were generated for each ligand. The best docking poses were selected based on binding affinity scores (kcal/mol) and analyzed for molecular interactions. The interactions, including hydrogen bonding, hydrophobic interactions, and other non-covalent interactions, were visualized and interpreted using Discovery Studio. The docking results were further compared with the native ligand to assess the binding efficiency and stability of the designed compounds. Active cavity of Human COX-2 with Native Ligand are shown in Figure 3.

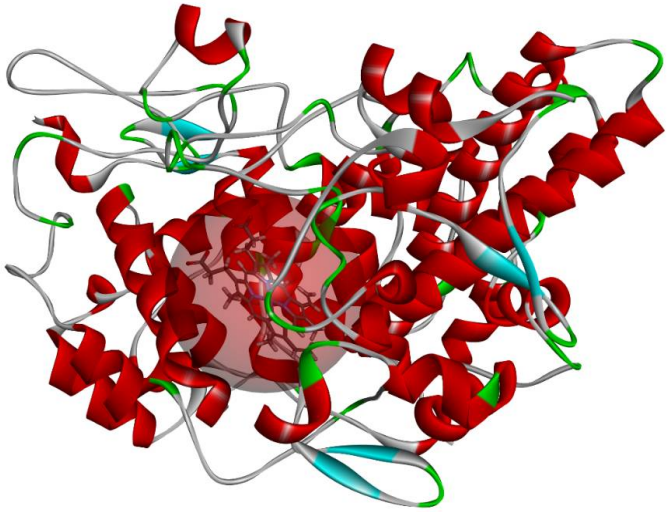

**Figure 3:** Active cavity of Human COX-2 with Native Ligand

**ADMET Analysis**

The pharmacokinetic and toxicity profiles of selected phytoconstituents from *Feronia elephantum* were evaluated using in silico ADMET analysis to assess their drug-likeness as potential Human COX-2 inhibitors. The chemical structures of the compounds were retrieved from PubChem and further drawn and optimized using ChemDraw to ensure structural accuracy. The prepared ligands were subjected to ADMET prediction using SwissADME and ADMETlab 3.0. Various physicochemical properties, including molecular weight, lipophilicity (LogP), hydrogen bond donors and acceptors, and topological polar surface area (TPSA), were analyzed to evaluate drug-likeness based on Lipinski's rule of five. Pharmacokinetic parameters such as gastrointestinal absorption, blood–brain barrier permeability, and bioavailability were predicted using SwissADME. Toxicological endpoints, including hepatotoxicity, carcinogenicity, mutagenicity, and acute toxicity, were assessed using ADMETlab 3.0. This integrated computational approach enabled the identification of compounds with favorable pharmacokinetic behavior and minimal toxicity, supporting their potential as safe and effective Human COX-2 inhibitors [27,28].

**RESULTS AND DISCUSSION**

**Organoleptic and Physicochemical Analysis of Extracts**

The hydroalcoholic extract of *Feronia elephantum* was evaluated for its organoleptic and physicochemical properties to establish its quality and standardization profile (Figure 4). The extract exhibited a brownish-black colour, mild aromatic odour, bitter and slightly sour taste, and a semi-solid texture. These characteristics suggest the presence of phytoconstituents such as tannins, flavonoids, and other phenolic

compounds, which are known to impart dark colour and astringency. The semi-solid nature indicates efficient extraction and concentration of bioactive compounds. The percentage yield (9.67%) reflects good extractability of constituents using a hydroalcoholic solvent system. The physicochemical analysis indicated that the extract is slightly acidic, with pH values of 5.9 (1% solution) and 4.5 (10% solution), likely due to the presence of organic acids and phenolic compounds. The low foreign matter content (0.5%) confirms minimal contamination and good quality of the raw material. The loss on drying value (7%) indicates acceptable moisture content, which is essential for stability and prevention of microbial growth. The ash values revealed moderate inorganic content, with total ash (8.8%) representing overall mineral composition and acid-insoluble ash (2.4%) indicating minimal siliceous impurities. The water-soluble ash (4.1%) suggests the presence of soluble inorganic salts, while the sulphated ash value (8%) confirms consistency of the inorganic residue. The extractive values showed a higher water-soluble fraction (22.81%) compared to the alcohol-soluble fraction (15.33%), indicating a predominance of polar constituents such as glycosides, tannins, and flavonoids. The absence of heavy metals and pesticide residues further confirms the safety and purity of the extract. Overall, these findings establish the quality, purity, and suitability of *Feronia elephantum* extract for further pharmacological investigation.

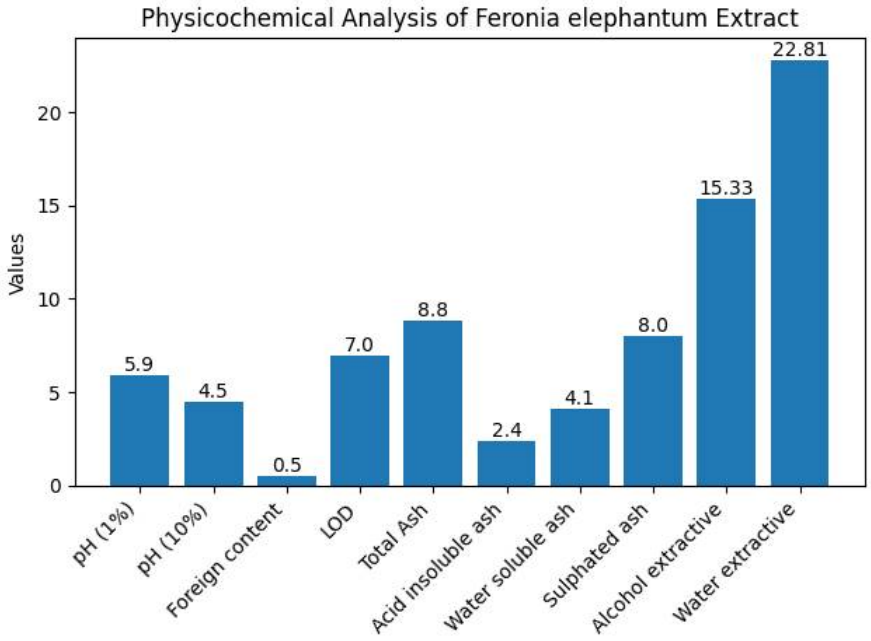


**Figure 4:** Physicochemical Analysis of *Feronia elephantum*

**Preliminary Phytochemical Screening of Extract**

Preliminary phytochemical screening of the hydroalcoholic extract of *Feronia elephantum* revealed the presence of a wide range of bioactive constituents, indicating its potential for therapeutic applications. The extract showed moderate presence of carbohydrates (++), along with trace amounts of reducing sugars and monosaccharides (+), suggesting the occurrence of both complex and simple sugar moieties that may contribute to metabolic and biological functions. Proteins were detected in low amounts (+), whereas amino acids were absent, indicating minimal contribution of free amino acids in the extract. A prominent presence of fats and oils (+++) was observed, indicating a high concentration of lipid-based constituents such as fatty acids and their derivatives, which are associated with anti-inflammatory and membrane-stabilizing properties. Steroids were moderately present (++), suggesting the presence of phytosterols that may contribute to anti-inflammatory and cholesterol-modulating effects. Cardiac glycosides and saponin glycosides were detected in trace amounts (+), indicating possible cardioprotective and surface-active properties. Anthraquinone glycosides were absent, suggesting that laxative-type constituents are not present in the extract. Alkaloids were detected in low amounts (+), indicating the presence of nitrogen-containing compounds that may contribute to pharmacological activity. Phenolic compounds, tannins, and flavonoids were moderately present (++), highlighting the antioxidant potential of the extract due to their well-established free radical scavenging activity. Overall, the phytochemical profile demonstrates that *Feronia elephantum* extract is rich in lipidic and phenolic constituents, along with moderate levels of steroids and glycosides. These bioactive components collectively contribute to the extract's potential pharmacological efficacy and support its further

investigation for therapeutic applications. Preliminary phytochemical screening of *Feronia elephantum* extract are shown in Figure 5.

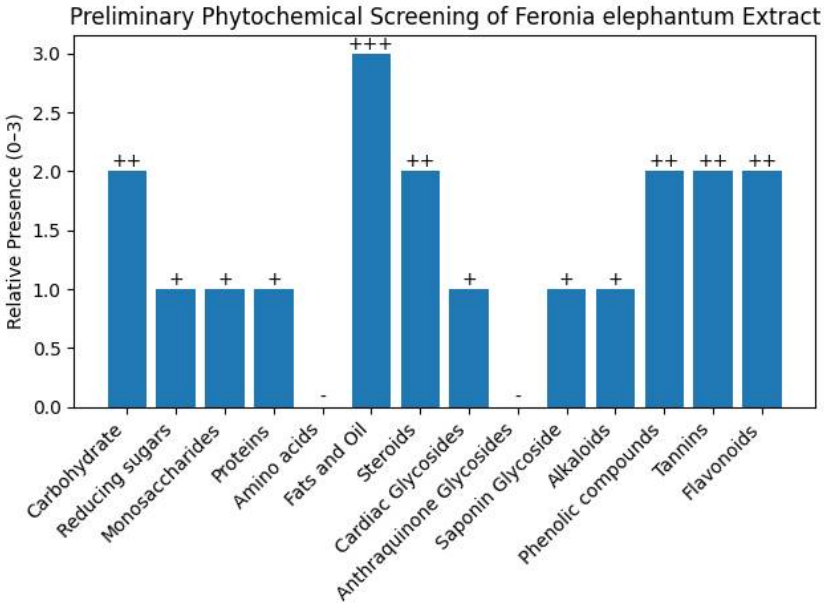


**Figure 5:** Preliminary phytochemical screening of *Feronia elephantum* extract

**Microbial Content Determination**

Microbial analysis of the *Feronia elephantum* extract showed the absence of all tested pathogens, including *Escherichia coli*, *Salmonella* spp., *Shigella* spp., *Pseudomonas aeruginosa*, and *Staphylococcus aureus*. This indicates that the extract is free from microbial contamination and meets acceptable safety standards. The absence of enteric and opportunistic pathogens reflects good hygienic practices during processing and extraction. Overall, the results confirm that the extract is microbiologically safe and suitable for further pharmacological applications.

**GC–MS Analysis**

The GC–MS analysis of *Feronia elephantum* extract revealed a complex mixture of volatile and semi-volatile phytoconstituents distributed across the chromatographic run (1–58 min), indicating the presence of compounds with varying polarity.

In the early retention time region, a major peak corresponding to Pentanoic acid, 3-methyl-4-oxo (RT 2.168 min, 10.34%) was observed, indicating it as a dominant low molecular weight compound. Other early to mid-retention compounds included 4H-Pyran-4-one, 2,3-dihydro-3,5-dihydroxy-6-methyl (RT 14.623 min, 0.29%), 4-Vinylphenol (RT 17.061 min, 0.42%), and 2-Methoxy-4-vinylphenol (RT 19.413 min, 0.11%), representing phenolic and oxygenated derivatives. Additionally, 2,4-Di-tert-butylphenol (RT 25.785 min, 0.21%) was identified as a phenolic antioxidant compound.

The mid-retention region showed the presence of moderately polar compounds such as Ethyl α-D-glucopyranoside (RT 29.864 min, 3.65%), indicating carbohydrate-derived constituents. In the late retention time region, non-polar compounds predominated, including Hexadecanoic acid, methyl ester (RT 34.120 min, 0.19%), n-Hexadecanoic acid (RT 34.731 min, 0.94%), 9,12-Octadecadienoic acid methyl ester (RT 36.498 min, 0.20%), and 6-Octadecenoic acid methyl ester (RT 36.609 min, 0.22%), representing fatty acids and their esters. Further, high molecular weight sterols and triterpenoids were detected at higher retention times, including Campesterol (RT 53.388 min, 1.14%), Ergosta-5,7-dien-3-ol (RT 53.780 min, 4.99%), Lanosta-8,24-dien-3-one (RT 54.373 min, 11.08%), 9,19-Cyclolanostan-3-ol, 24-methylene (RT 55.192 min, 8.43%), and 9,19-Cyclolanost-23-ene-3,25-diol (RT 55.353 min, 12.20%), indicating the dominance of triterpenoid and sterol constituents in the extract. Overall, the GC–MS results confirmed the presence of diverse phytoconstituents including phenolics, fatty acids, sterols, and triterpenoids, with major contributions from cyclolanostane-type compounds (Table 1). The graph of GCMS analysis is shown in Figure 6.

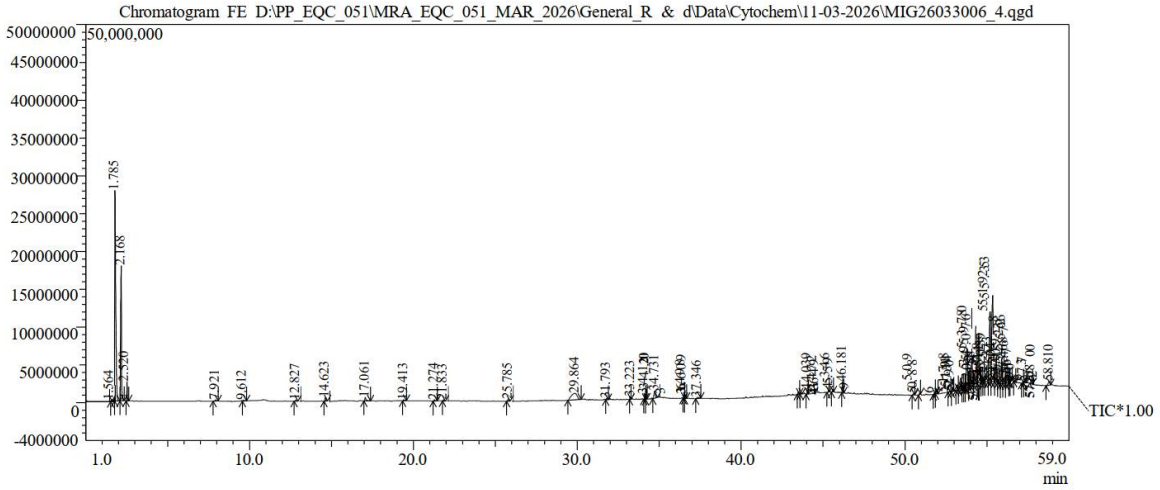


Figure 6: The Graph of GCMS Analysis

Table 1: Compound identified in GC-MS Analysis for *Feronia elephantum*

| Sr. No. | Peak RT (min) | Area % | Suggested Compound | Compound Code |
|---|---|---|---|---|
| 1 | 25.785 | 0.21 | 2,4-Di-tert-butylphenol | FE-01 |
| 2 | 19.413 | 0.11 | 2-Methoxy-4-vinylphenol | FE-02 |
| 3 | 14.623 | 0.29 | 4H-Pyran-4-one, 2,3-dihydro-3,5-dihydroxy-6-methyl | FE-03 |
| 4 | 17.061 | 0.42 | 4-Vinylphenol | FE-04 |
| 5 | 36.609 | 0.22 | 6-Octadecenoic acid, methyl ester | FE-05 |
| 6 | 36.498 | 0.20 | 9,12-Octadecadienoic acid (Z,Z)-, methyl ester | FE-06 |
| 7 | 55.353 | 12.20 | 9,19-Cyclolanost-23-ene-3,25-diol | FE-07 |
| 8 | 55.192 | 8.43 | 9,19-Cyclolanostan-3-ol, 24-methylene | FE-08 |
| 9 | 53.388 | 1.14 | Campesterol | FE-09 |
| 10 | 53.780 | 4.99 | Ergosta-5,7-dien-3-ol | FE-10 |
| 11 | 29.864 | 3.65 | Ethyl α-D-glucopyranoside | FE-11 |
| 12 | 34.120 | 0.19 | Hexadecanoic acid, methyl ester | FE-12 |
| 13 | 54.373 | 11.08 | Lanosta-8,24-dien-3-one | FE-13 |
| 14 | 34.731 | 0.94 | n-Hexadecanoic acid | FE-14 |
| 15 | 2.168 | 10.34 | Pentanoic acid, 3-methyl-4-oxo | FE-15 |

## Molecular Docking

Molecular docking analysis was performed to evaluate the binding affinity and interaction profile of selected phytoconstituents (FE-01 to FE-15) with Human COX-2 (PDB ID: 5KIR), using Rofecoxib as the reference standard. Rofecoxib exhibited a docking score of −8.0 kcal/mol with a ligand energy of 634.73 kcal/mol, forming a key conventional hydrogen bond with GLN203 (2.79 Å) along with significant hydrophobic interactions involving VAL295, LEU391, and ILE408. These interactions confirm its stable binding within the active site and serve as a benchmark for comparison. Among the tested compounds, several phytoconstituents demonstrated binding affinities comparable to or exceeding that of Rofecoxib. Notably, FE-09 (−8.7 kcal/mol) showed the highest binding affinity, followed by FE-10 (−8.5 kcal/mol), FE-13 (−8.1 kcal/mol), and FE-15 (−8.1 kcal/mol). These compounds exhibited extensive hydrophobic interactions with key active site residues such as LEU294, VAL447, VAL295, LEU391, and ILE408, which are crucial for COX-2 inhibition. The dominance of hydrophobic interactions suggests strong stabilization within the enzyme's binding pocket, similar to or better than Rofecoxib. Importantly, FE-15 demonstrated a highly stable binding pattern through multiple conventional hydrogen bonds with HIS207 (2.27 Å), ASN382 (2.22 Å), and HIS386 (2.42 Å), along with additional electrostatic (Pi–cation) and hydrophobic interactions. This multi-interaction profile indicates stronger and more stable binding compared to Rofecoxib. Likewise, FE-13 formed a significant hydrogen bond with THR212 (2.05 Å) along with multiple hydrophobic contacts, contributing to its comparable docking score relative to Rofecoxib.

Compounds such as FE-05 (−6.5 kcal/mol), FE-02 (−6.2 kcal/mol), FE-01 and FE-04 (−6.1 kcal/mol), and FE-11 (−6.3 kcal/mol) exhibited moderate binding affinity when compared with Rofecoxib. These compounds formed limited hydrogen bonds and fewer hydrophobic interactions, indicating relatively lower binding stability within the COX-2 active site. In contrast, FE-03, FE-06, FE-12, and FE-14 showed lower docking scores ranging from −5.7 to −5.9 kcal/mol, indicating weaker binding interactions

compared to Rofecoxib. Although some hydrogen bonding interactions were observed (e.g., with TYR385 and ASN382), the overall interaction network was insufficient to achieve strong stabilization within the binding pocket.

Overall, the docking results clearly indicate that several phytoconstituents, particularly FE-09, FE-10, FE-13, and FE-15, exhibit binding affinities comparable to or better than Rofecoxib, supported by strong hydrophobic interactions and key hydrogen bonding within the COX-2 active site. These findings suggest that these compounds may act as potential COX-2 inhibitors and could be considered for further pharmacological evaluation. Binding interactions of selected compounds with Human COX-2 are shown in Table 2. **2**D and 3D Binding Interaction most potent compound with Human COX-2 are shown in Table 3.

**Table 2: Binding interactions of selected compounds with Human COX-2**

| Amino Acid | Bond Length | Bond Type | Bond Category | Ligand Energy | Docking Score |
|---|---|---|---|---|---|
| | | | | (Kcal/mol) | |
| Rofecoxib-NL | | | | | |
| GLN203 | 2.7978 | Hydrogen Bond | Conventional Hydrogen Bond | 634.73 | -8 |
| VAL295 | 3.57476 | Hydrophobic | Pi-Sigma | | |
| LEU391 | 3.97912 | | | | |
| ILE408 | 4.29111 | | Pi-Alkyl | | |
| FE-01 | | | | | |
| THR206 | 2.87135 | Hydrogen Bond | Conventional Hydrogen Bond | 109.26 | -6.1 |
| HIS388 | 3.69631 | Hydrophobic | Pi-Sigma | | |
| HIS386 | 3.90107 | | | | |
| HIS207 | 4.33172 | | Pi-Pi T-shaped | | |
| HIS207 | 4.92922 | | Pi-Alkyl | | |
| HIS207 | 5.18592 | | | | |
| HIS386 | 4.38658 | | | | |
| HIS388 | 4.49825 | | | | |
| FE-02 | | | | | |
| TYR385 | 2.41028 | Hydrogen Bond | Conventional Hydrogen Bond | 81.23 | -6.2 |
| TYR385 | 3.75489 | | Carbon Hydrogen Bond | | |
| GLN203 | 4.24808 | Hydrophobic | Amide-Pi Stacked | | |
| ALA199 | 4.37548 | | Alkyl | | |
| LEU391 | 4.60348 | | | | |
| ALA202 | 4.58543 | | Pi-Alkyl | | |
| FE-03 | | | | | |
| TYR385 | 2.46551 | Hydrogen Bond | Conventional Hydrogen Bond | 108.35 | -5.7 |
| ALA199 | 2.75639 | | | | |
| HIS207 | 3.56018 | | Carbon Hydrogen Bond | | |
| LEU391 | 4.53935 | Hydrophobic | Alkyl | | |
| HIS388 | 5.14608 | | Pi-Alkyl | | |
| FE-04 | | | | | |
| GLN203 | 4.12458 | Hydrophobic | Amide-Pi Stacked | 53.77 | -6.1 |
| ALA199 | 4.27893 | | Alkyl | | |
| LEU391 | 4.58311 | | | | |
| ALA202 | 4.3788 | | Pi-Alkyl | | |
| FE-05 | | | | | |
| ILE408 | 3.97742 | Hydrophobic | Alkyl | 11.22 | -6.5 |
| TYR404 | 5.41158 | | Pi-Alkyl | | |

| | | | | | |
|---|---|---|---|---|---|
| FE-06 | | | | | |
| TYR385 | 3.3991 | Hydrogen Bond | Carbon Hydrogen Bond | 11.81 | -5.9 |
| ILE408 | 3.78478 | Hydrophobic | Alkyl | | |
| TYR404 | 5.31522 | | Pi-Alkyl | | |
| FE-07 | | | | | |
| VAL447 | 4.89447 | Hydrophobic | Alkyl | 1660.1 | -7.1 |
| VAL447 | 4.6342 | | | | |
| VAL447 | 4.4776 | | | | |
| LEU294 | 4.38591 | | | | |
| HIS207 | 4.8706 | | Pi-Alkyl | | |
| HIS207 | 5.22291 | | | | |
| HIS386 | 4.15869 | | | | |
| HIS386 | 4.83865 | | | | |
| FE-08 | | | | | |
| VAL291 | 4.51946 | Hydrophobic | Alkyl | 1759.01 | -7.5 |
| VAL291 | 4.65638 | | | | |
| VAL447 | 3.95272 | | | | |
| LEU294 | 4.02444 | | | | |
| VAL447 | 4.09901 | | | | |
| LEU294 | 4.94246 | | | | |
| LEU391 | 4.68401 | | | | |
| VAL295 | 3.87515 | | | | |
| LEU391 | 4.56016 | | | | |
| VAL295 | 4.47191 | | | | |
| LEU391 | 4.80158 | | | | |
| LEU294 | 5.48343 | | | | |
| PHE200 | 5.01779 | | Pi-Alkyl | | |
| HIS207 | 5.4853 | | | | |
| HIS207 | 4.70465 | | | | |
| HIS207 | 4.01723 | | | | |
| HIS214 | 5.3065 | | | | |
| HIS388 | 5.09918 | | | | |
| HIS388 | 4.69106 | | | | |
| PHE395 | 5.11418 | | | | |
| TYR404 | 4.67078 | | | | |
| FE-09 | | | | | |
| LEU294 | 5.37193 | Hydrophobic | Alkyl | 404.31 | -8.7 |
| VAL447 | 3.9716 | | | | |
| LEU294 | 4.7775 | | | | |
| LEU294 | 4.28494 | | | | |
| ILE408 | 4.9318 | | | | |
| VAL444 | 5.20356 | | | | |
| VAL295 | 4.13893 | | | | |
| LEU391 | 4.49541 | | | | |
| VAL295 | 4.40648 | | | | |

| | | | | | |
|---|---|---|---|---|---|
| LEU391 | 4.81736 | | | | |
| HIS207 | 5.46115 | | | | |
| HIS207 | 4.97164 | | | | |
| HIS214 | 4.81297 | | | | |
| HIS388 | 4.73876 | | Pi-Alkyl | | |
| PHE395 | 4.75425 | | | | |
| TYR404 | 5.23457 | | | | |
| TYR404 | 4.58315 | | | | |
| FE-10 | | | | | |
| LEU294 | 4.29933 | | | | |
| VAL447 | 3.92074 | | | | |
| VAL444 | 5.19775 | | | | |
| VAL447 | 5.12453 | | | | |
| LEU391 | 4.74994 | | | | |
| VAL444 | 4.75271 | | Alkyl | | |
| VAL295 | 4.02301 | | | | |
| LEU391 | 4.48265 | | | | |
| VAL295 | 4.4671 | | | | |
| LEU391 | 4.802 | Hydrophobic | | 2593.78 | -8.5 |
| VAL447 | 4.57788 | | | | |
| PHE200 | 5.2041 | | | | |
| HIS207 | 4.75655 | | | | |
| HIS207 | 5.25779 | | | | |
| HIS386 | 4.96496 | | | | |
| HIS388 | 5.254 | | Pi-Alkyl | | |
| HIS388 | 4.63527 | | | | |
| HIS388 | 4.72418 | | | | |
| PHE395 | 4.84476 | | | | |
| TYR404 | 4.55359 | | | | |
| FE-11 | | | | | |
| ALA199 | 2.95581 | | | | |
| HIS207 | 2.05438 | | Conventional Hydrogen Bond | | |
| ALA202 | 2.46147 | Hydrogen Bond | | 520.12 | -6.3 |
| THR206 | 2.05895 | | | | |
| HIS388 | 3.45625 | | Carbon Hydrogen Bond | | |
| HIS388 | 5.05992 | Hydrophobic | Pi-Pi T-shaped | | |
| FE-12 | | | | | |
| TYR148 | 3.05111 | | Conventional Hydrogen Bond | | |
| THR212 | 2.57631 | Hydrogen Bond | | | |
| ASN382 | 3.50735 | | Carbon Hydrogen Bond | | |
| ALA199 | 4.00069 | | Alkyl | 13.61 | -5.9 |
| LEU391 | 4.83623 | Hydrophobic | | | |
| PHE200 | 4.42322 | | Pi-Alkyl | | |
| FE-13 | | | | | |
| THR212 | 2.05961 | Hydrogen Bond | Conventional Hydrogen Bond | 423.94 | -8.1 |

| | | | | | |
|---|---|---|---|---|---|
| HIS207 | 3.8355 | Hydrophobic | Pi-Sigma | | |
| LEU294 | 4.77009 | | Alkyl | | |
| VAL444 | 5.20254 | | | | |
| VAL447 | 3.83787 | | | | |
| LEU294 | 3.91394 | | | | |
| VAL447 | 5.47582 | | | | |
| LEU294 | 4.5062 | | | | |
| VAL295 | 4.47734 | | | | |
| VAL295 | 4.8821 | | | | |
| LEU391 | 4.39798 | | | | |
| VAL447 | 4.77549 | | | | |
| HIS207 | 4.93755 | | Pi-Alkyl | | |
| HIS214 | 5.35638 | | | | |
| HIS386 | 4.34073 | | | | |
| HIS388 | 5.33561 | | | | |
| HIS388 | 4.91758 | | | | |
| PHE395 | 5.37075 | | | | |
| TYR404 | 4.61821 | | | | |
| FE-14 | | | | | |
| ASN382 | 2.55988 | Hydrogen Bond | Conventional Hydrogen Bond | 2.1 | -5.8 |
| HIS386 | 2.9156 | | | | |
| VAL295 | 4.51105 | Hydrophobic | Alkyl | | |
| LEU391 | 4.60287 | | | | |
| PHE395 | 5.07781 | | Pi-Alkyl | | |
| TYR404 | 4.7309 | | | | |
| FE-15 | | | | | |
| HIS207 | 2.27471 | Hydrogen Bond | Conventional Hydrogen Bond | 355.51 | -8.1 |
| ASN382 | 2.22109 | | | | |
| HIS386 | 2.42586 | | | | |
| GLN289 | 3.58895 | | Carbon Hydrogen Bond | | |
| LYS211 | 3.23407 | | | | |
| HIS386 | 3.3174 | | | | |
| HIS386 | 4.73061 | Electrostatic | Pi-Cation | | |
| VAL291 | 3.77966 | Hydrophobic | Pi-Sigma | | |
| HIS214 | 4.95947 | Other | Pi-Sulfur | | |
| LYS211 | 4.07052 | Hydrophobic | Alkyl | | |
| VAL291 | 4.72121 | | | | |

**Table 3: 2D and 3D Binding Interaction most potent compound with Human COX-2**

| 3D Binding Interaction | 2D Binding Interaction |
|---|---|
| **Rofecoxib-NL** | |
| 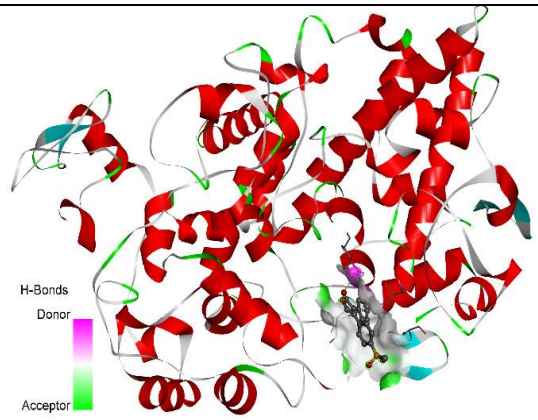  | 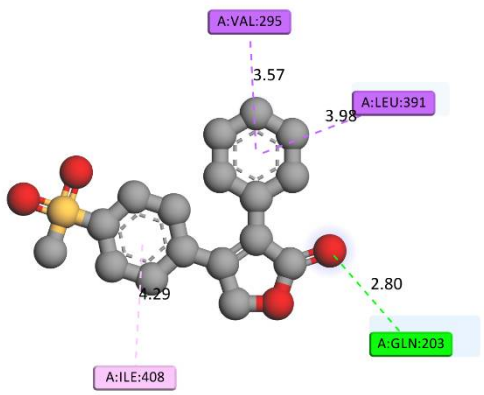  |
| **FE-01** | |

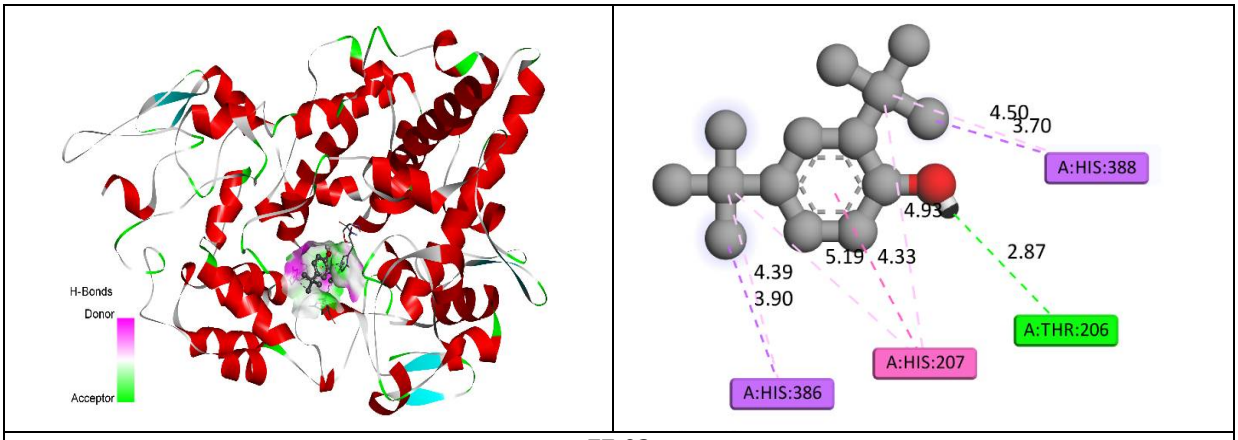


**FE-02**

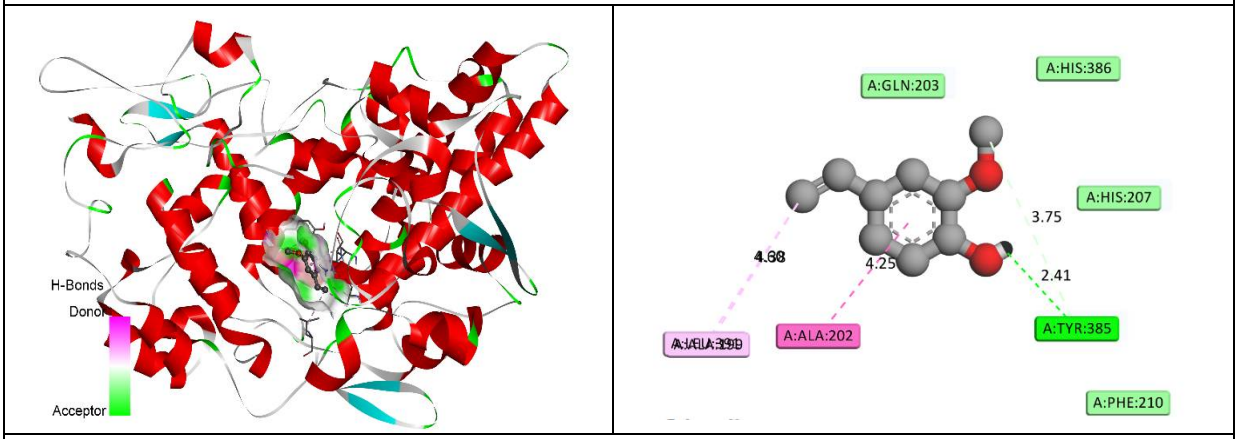


**FE-03**

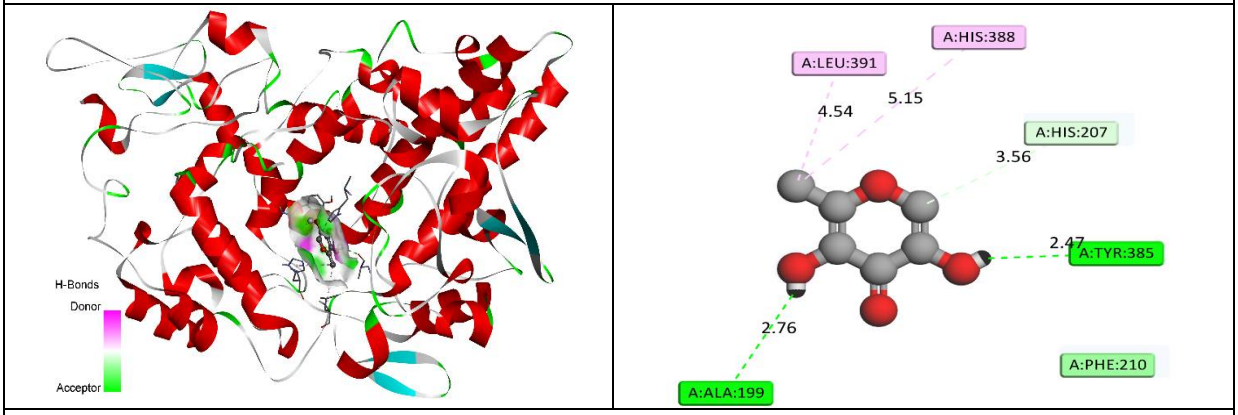


**FE-04**

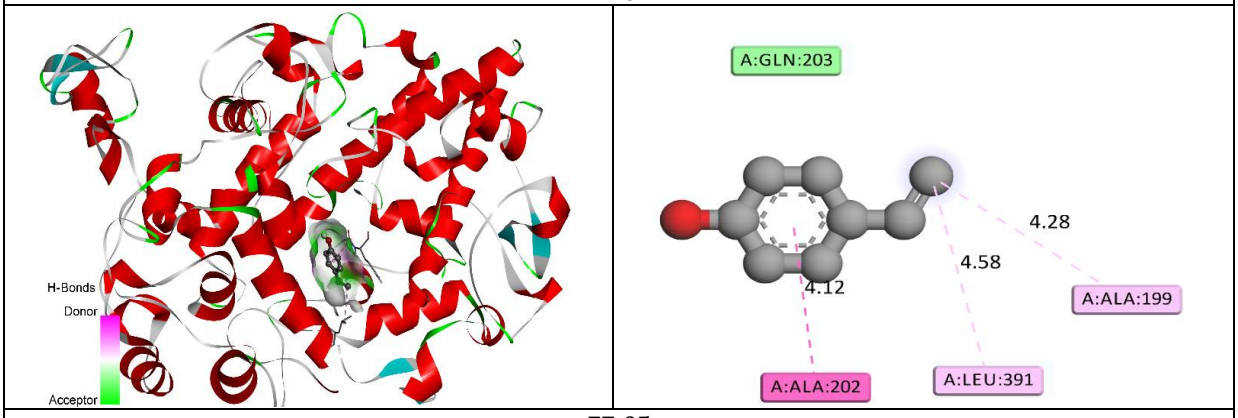


**FE-05**

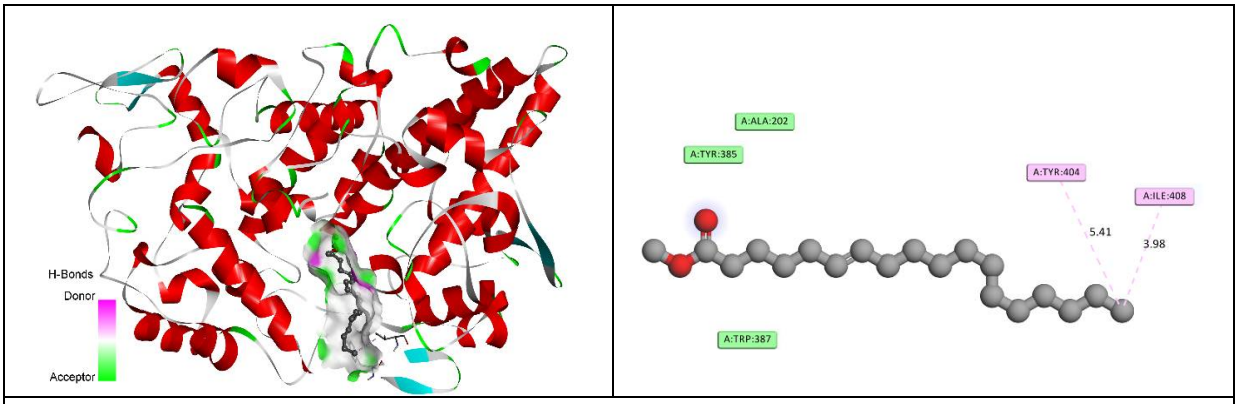


**FE-06**

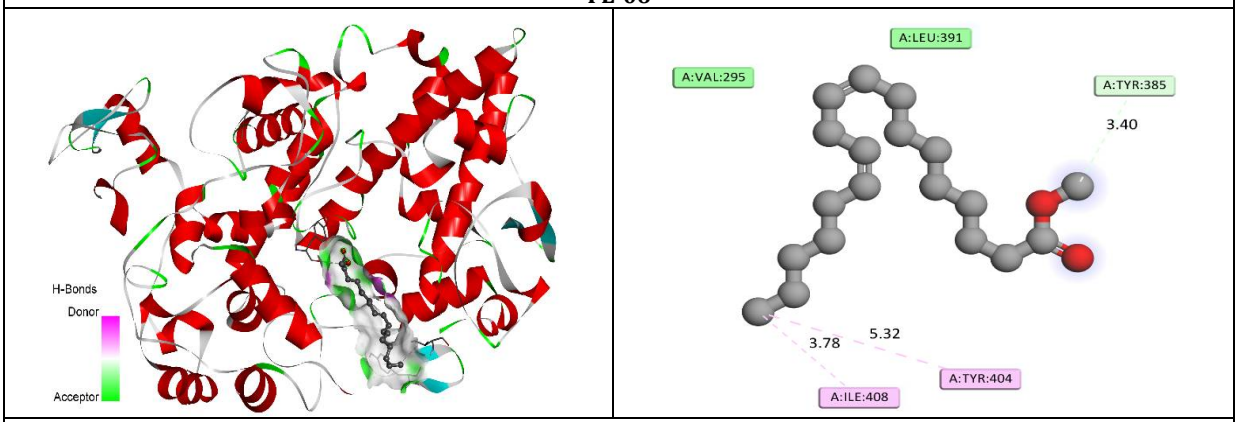


**FE-07**

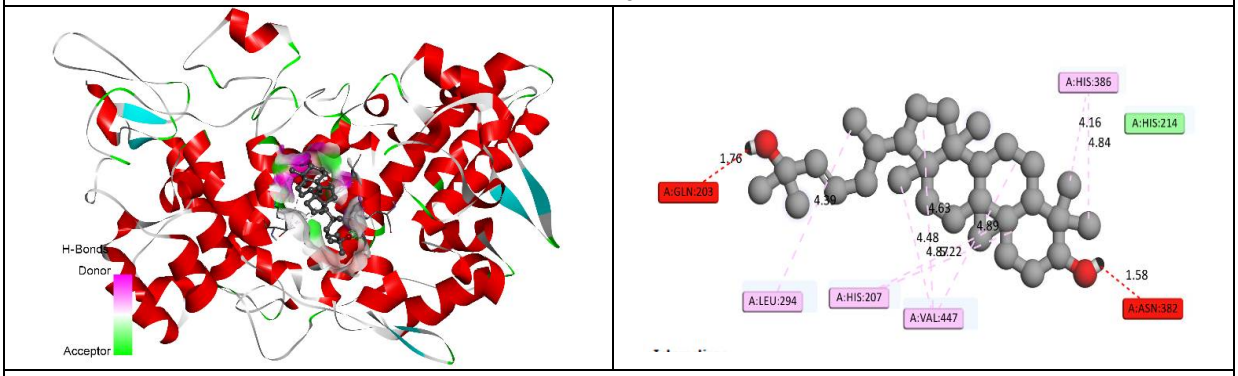


**FE-08**

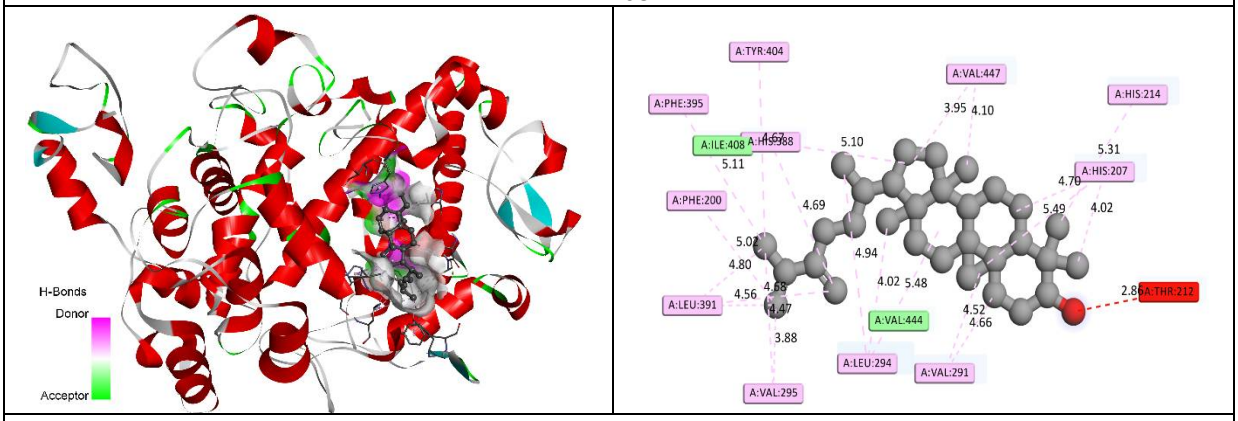


**FE-09**

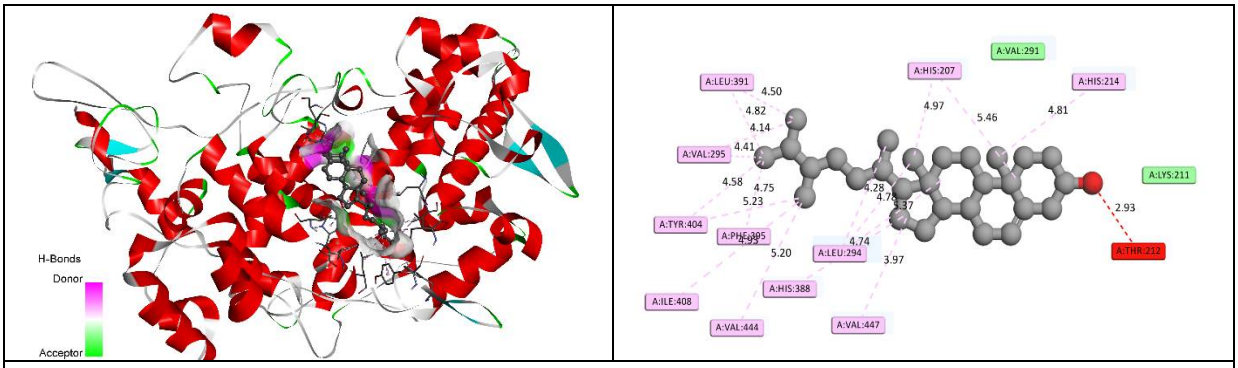


**FE-10**

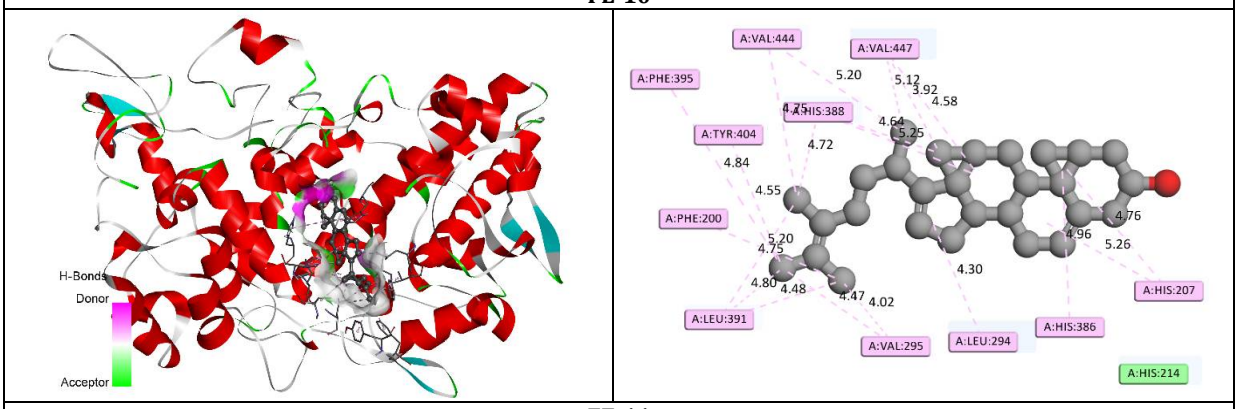


**FE-11**

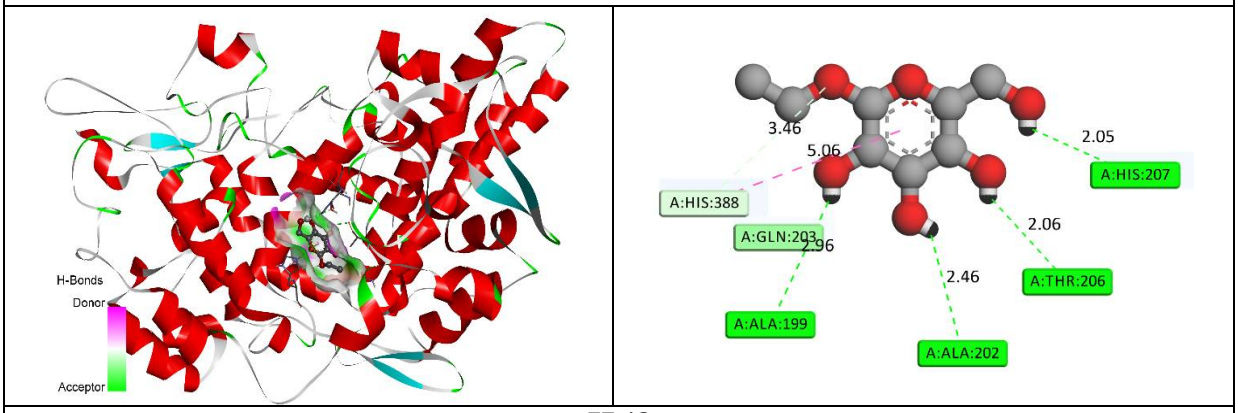


**FE-12**

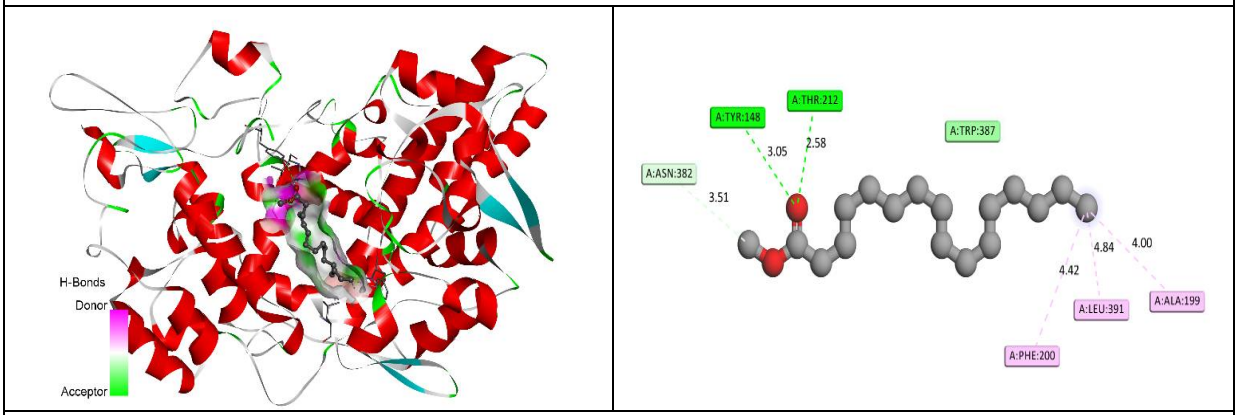


**FE-13**

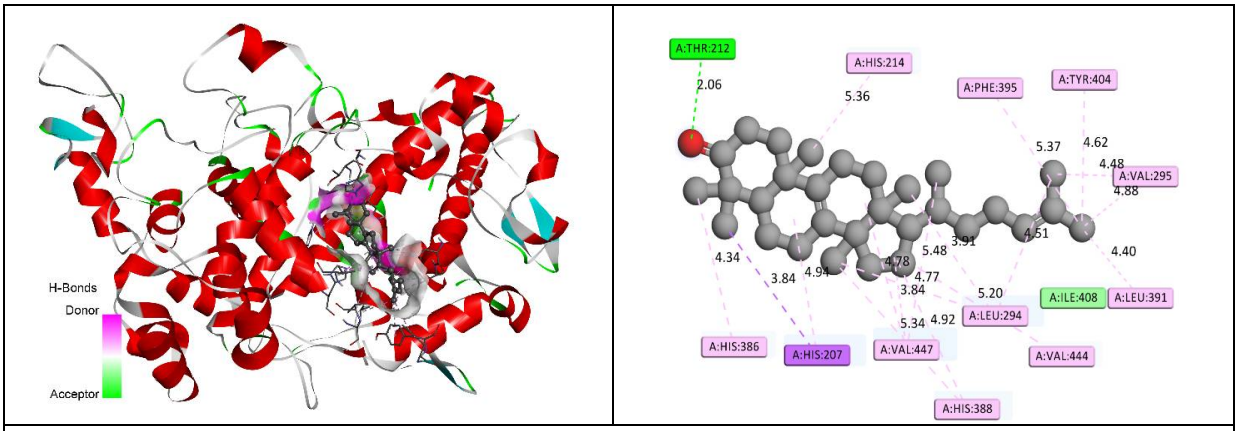


**FE-14**

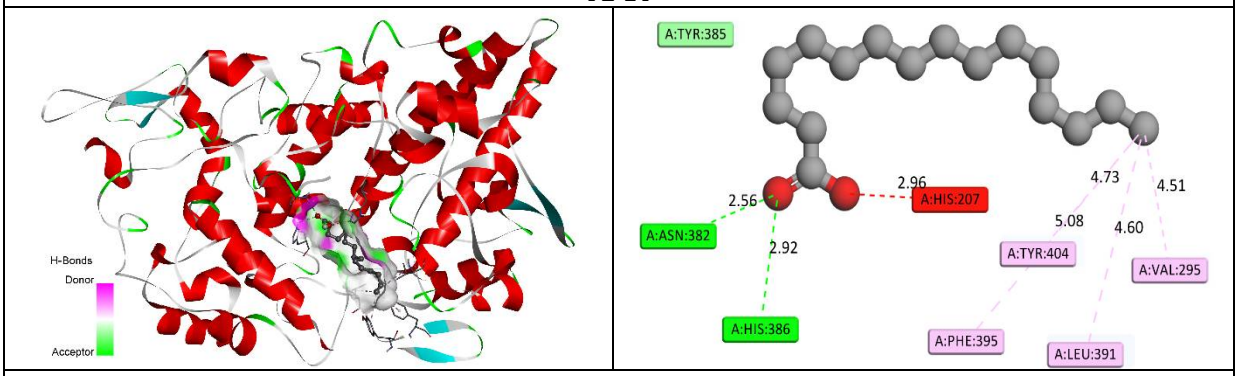


**FE-15**

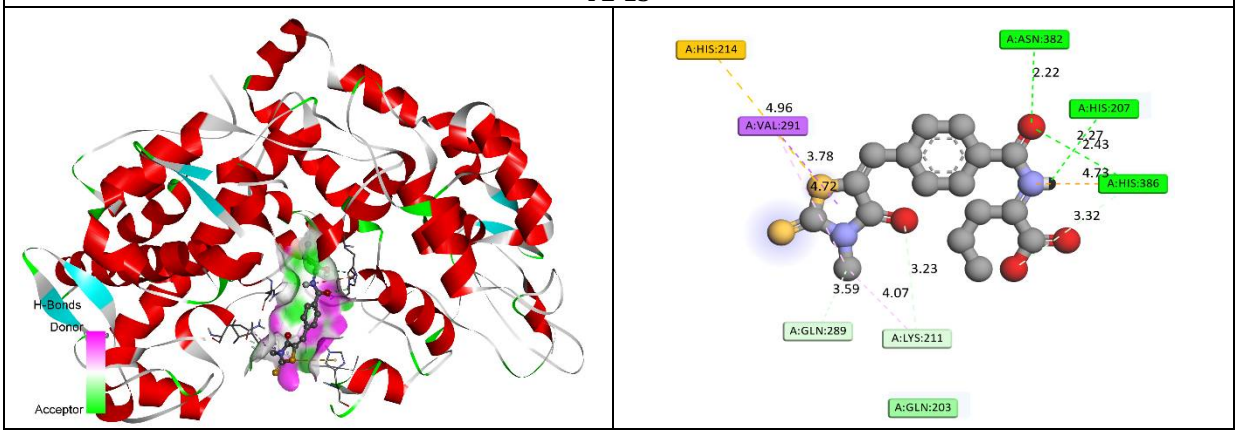


## ADMET Analysis

The ADMET and physicochemical properties of the selected compounds (FE-01 to FE-15) were evaluated and compared with Rofecoxib, which was used as the reference standard (Table 4). Rofecoxib exhibited favorable drug-like characteristics, including moderate molecular weight (314.06 g/mol), balanced lipophilicity (logP 1.64), and acceptable solubility (logS −3.18), indicating good oral bioavailability and permeability. Among the screened compounds, FE-02, FE-03, FE-04, and FE-01 demonstrated lower molecular weights with moderate lipophilicity and low TPSA values, suggesting good membrane permeability and absorption potential comparable to Rofecoxib. In particular, FE-02 and FE-04 showed a favorable balance between solubility and lipophilicity, indicating suitable pharmacokinetic behavior. Conversely, long-chain derivatives such as FE-05, FE-06, FE-12, and FE-14 exhibited very high lipophilicity (logP > 6) and poor solubility (logS < −5), which may adversely affect their bioavailability despite good permeability. Similarly, sterol and triterpenoid compounds (FE-07, FE-08, FE-09, FE-10, and FE-13) showed higher molecular weights and increased hydrophobicity, which could limit their pharmacokinetic performance even though they demonstrated strong docking affinity.

Compound FE-11 displayed high polarity with elevated TPSA (99.38 $Å^2$) and multiple hydrogen bonding sites, resulting in good solubility but potentially reduced membrane permeability due to low lipophilicity

(logP −1.58). Notably, FE-15 exhibited a well-balanced ADMET profile, with moderate molecular weight, acceptable TPSA, and optimal lipophilicity (logP 1.09) along with reasonable solubility, closely resembling the pharmacokinetic characteristics of Rofecoxib.

Overall, while several compounds showed promising binding affinity in docking studies, only a few exhibited balanced ADMET properties comparable to Rofecoxib. Among them, FE-15, followed by FE-02 and FE-04, emerged as potential candidates with favorable drug-likeness and pharmacokinetic profiles, supporting their suitability for further drug development studies.

**Table 4: Physicochemical properties of selected derivatives**

| Compounds | MW | Volume | Dense | nHA | nHD | nRot | nRing | TPSA | logS | logP |
|---|---|---|---|---|---|---|---|---|---|---|
| Rofecoxib-NL | 314.06 | 309.4971 | 1.014743 | 4 | 0 | 3 | 3 | 60.44 | -3.18942 | 1.641552 |
| FE-01 | 206.17 | 243.0246 | 0.84835 | 1 | 1 | 2 | 1 | 20.23 | -4.28379 | 4.606541 |
| FE-02 | 150.07 | 162.6985 | 0.922381 | 2 | 1 | 2 | 1 | 29.46 | -1.63923 | 2.052078 |
| FE-03 | 144.04 | 133.6639 | 1.077628 | 4 | 2 | 0 | 1 | 66.76 | -0.07523 | -0.73039 |
| FE-04 | 120.06 | 136.6123 | 0.878838 | 1 | 1 | 1 | 1 | 20.23 | -0.95618 | 1.992716 |
| FE-05 | 296.27 | 349.4877 | 0.847727 | 2 | 0 | 16 | 0 | 26.3 | -7.23903 | 7.425875 |
| FE-06 | 294.26 | 346.8513 | 0.848375 | 2 | 0 | 15 | 0 | 26.3 | -6.57696 | 7.012045 |
| FE-07 | 442.38 | 499.5977 | 0.885472 | 2 | 2 | 4 | 5 | 40.46 | -5.0489 | 4.549424 |
| FE-08 | 440.4 | 508.1035 | 0.866753 | 1 | 1 | 5 | 5 | 20.23 | -7.59689 | 7.352299 |
| FE-09 | 400.37 | 464.772 | 0.861433 | 1 | 1 | 5 | 4 | 20.23 | -6.92787 | 7.662918 |
| FE-10 | 398.35 | 462.1355 | 0.861977 | 1 | 1 | 5 | 4 | 20.23 | -6.37803 | 7.030876 |
| FE-11 | 208.09 | 191.1092 | 1.088854 | 6 | 4 | 3 | 1 | 99.38 | -0.0035 | -1.58452 |
| FE-12 | 270.26 | 317.5322 | 0.851126 | 2 | 0 | 15 | 0 | 26.3 | -7.0315 | 7.287134 |
| FE-13 | 424.37 | 494.091 | 0.85889 | 1 | 0 | 4 | 4 | 17.07 | -6.4493 | 6.683897 |
| FE-14 | 256.24 | 300.2362 | 0.853461 | 2 | 1 | 14 | 0 | 37.3 | -5.69319 | 6.647652 |
| FE-15 | 378.07 | 358.5561 | 1.054424 | 6 | 2 | 7 | 2 | 86.71 | -3.18892 | 1.090174 |

The drug-likeness properties of the selected compounds (FE-01 to FE-15) were evaluated and compared with Rofecoxib as the reference standard (Table 5). Rofecoxib exhibited a high quantitative estimate of drug-likeness (QED = 0.817) with no violations of Lipinski, Pfizer, GSK, Golden Triangle, or Chelator rules, indicating an optimal balance of physicochemical and pharmacokinetic properties. Its NP score (−0.07) suggests moderate natural product likeness with good drug-like characteristics.

Among the tested compounds, FE-02 (QED = 0.699) and FE-01 (QED = 0.68) demonstrated relatively high drug-likeness scores, approaching that of Rofecoxib. Notably, FE-02 showed a positive NP score (1.011) along with compliance to Lipinski, Pfizer, and GSK rules, while also satisfying the Golden Triangle and Chelator rules, indicating a well-balanced profile for drug development. Similarly, FE-04 (QED = 0.601) and FE-15 (QED = 0.584) exhibited moderate drug-likeness with no major rule violations, suggesting favorable pharmacokinetic potential comparable to Rofecoxib. Compounds such as FE-03 (QED = 0.491) and FE-10 (QED = 0.506) showed moderate drug-likeness, supported by positive NP scores, indicating their similarity to natural bioactive compounds. However, their slightly lower QED values suggest less optimal balance compared to Rofecoxib. In contrast, sterol and triterpenoid derivatives including FE-07, FE-08, FE-09, and FE-13 exhibited high NP scores (> 2.5), reflecting strong natural product characteristics. However, these compounds showed lower QED values (0.41–0.47) and multiple violations of Pfizer and GSK rules, indicating potential limitations in drug-likeness despite their biological relevance. Compounds FE-05, FE-06, FE-12, and FE-14 demonstrated low QED values (0.20–0.30) along with multiple rule violations, suggesting poor drug-likeness and limited suitability for further drug development. Importantly, all compounds satisfied Lipinski's rule of five (no violations), indicating acceptable basic drug-like properties such as molecular weight, hydrogen bonding capacity, and lipophilicity.

Overall, when compared with Rofecoxib, compounds FE-02, FE-01, FE-04, and FE-15 exhibited the most favorable drug-likeness profiles with minimal rule violations and balanced QED values. Among these, FE-02 and FE-15 emerge as promising candidates due to their optimal combination of drug-likeness, natural

product characteristics, and compliance with key pharmacokinetic rules, supporting their potential for further development as therapeutic agents.

**Table 5: Drug-likeness properties of designed derivatives**

| Compounds | QED | NP Score | Lipinski rule | Pfizer Rule | GSK Rule | Golden Triangle | Chelator Rule |
|---|---|---|---|---|---|---|---|
| Rofecoxib-NL | 0.817 | -0.07 | 0 | 0 | 0 | 0 | 0 |
| FE-01 | 0.68 | -0.064 | 0 | 1 | 1 | 0 | 0 |
| FE-02 | 0.699 | 1.011 | 0 | 0 | 0 | 1 | 1 |
| FE-03 | 0.491 | 1.665 | 0 | 0 | 0 | 1 | 0 |
| FE-04 | 0.601 | 0.864 | 0 | 0 | 0 | 1 | 0 |
| FE-05 | 0.204 | 0.727 | 0 | 1 | 1 | 0 | 0 |
| FE-06 | 0.224 | 1.03 | 0 | 1 | 1 | 0 | 0 |
| FE-07 | 0.454 | 3.396 | 0 | 1 | 1 | 0 | 0 |
| FE-08 | 0.425 | 3.267 | 0 | 1 | 1 | 1 | 0 |
| FE-09 | 0.47 | 2.676 | 0 | 1 | 1 | 1 | 0 |
| FE-10 | 0.506 | 2.876 | 0 | 1 | 1 | 0 | 0 |
| FE-11 | 0.421 | 2.348 | 0 | 0 | 0 | 0 | 0 |
| FE-12 | 0.301 | 0.253 | 0 | 1 | 1 | 0 | 0 |
| FE-13 | 0.412 | 3.382 | 0 | 1 | 1 | 0 | 0 |
| FE-14 | 0.413 | 0.385 | 0 | 1 | 1 | 0 | 0 |
| FE-15 | 0.584 | -1.194 | 0 | 0 | 0 | 0 | 0 |

The absorption-related ADMET parameters of the selected compounds (FE-01 to FE-15) were evaluated and compared with Rofecoxib as the reference standard (Table 6). Rofecoxib exhibited moderate permeability with Caco-2 (−4.71) and MDCK (−4.56) values, along with negligible P-glycoprotein (P-gp) substrate probability and low human intestinal absorption (HIA), indicating controlled absorption and limited efflux liability.

Among the tested compounds, FE-01 and FE-02 demonstrated permeability values comparable to Rofecoxib, suggesting favorable intestinal absorption. Notably, FE-01 showed a high probability of P-gp inhibition (0.97), which may enhance intracellular drug retention, although its moderate P-gp substrate nature indicates partial efflux susceptibility. Similarly, FE-02 exhibited balanced permeability with moderate absorption probabilities (F20%, F30%, and F50%), indicating acceptable oral bioavailability. Compounds such as FE-03 and FE-04 showed slightly improved Caco-2 permeability but higher P-gp substrate probability (especially FE-03), suggesting that efflux mechanisms may limit their effective absorption despite reasonable permeability.

Highly lipophilic compounds including FE-05, FE-06, FE-07, FE-08, FE-09, and FE-10 generally exhibited lower permeability (more negative Caco-2 values) and variable P-gp interactions. For instance, FE-08 and FE-13 showed high P-gp inhibition potential, which may enhance retention but could also lead to drug–drug interaction risks. However, these compounds displayed very low HIA values, indicating poor intestinal absorption despite favorable bioavailability fractions at higher thresholds (F50%). Interestingly, FE-12 and FE-14 demonstrated relatively higher HIA values (0.55 and 0.84, respectively), indicating good intestinal absorption compared to Rofecoxib. Additionally, FE-14 showed minimal P-gp inhibition and substrate interaction, suggesting reduced efflux and better absorption efficiency. FE-11 exhibited the lowest permeability (Caco-2 −5.76) but relatively higher HIA (0.38), indicating that alternative transport mechanisms may contribute to its absorption. Importantly, FE-15 demonstrated a balanced absorption profile with moderate permeability (Caco-2 −5.08, MDCK −4.85), low P-gp substrate probability, and acceptable HIA (0.19). Additionally, its high bioavailability fraction at F50% (0.99) suggests efficient systemic availability at higher doses, comparable or superior to Rofecoxib.

Overall, compared to Rofecoxib, compounds FE-01, FE-02, FE-12, FE-14, and FE-15 exhibited relatively favorable absorption characteristics. Among these, FE-14 and FE-15 stand out due to their improved HIA, balanced permeability, and minimal efflux liability, indicating their potential as promising candidates with enhanced oral absorption profiles.

**Table 6: Absorption parameter of selected compounds**

| Compounds | Caco-2 Permeability | MDCK Permeability | Pgp-inhibitor | Pgp-substrate | HIA | F20% | F30% | F50% |
|---|---|---|---|---|---|---|---|---|
| Rofecoxib-NL | -4.71569 | -4.5641 | 0.341514 | 0.00011 | 0.000567 | 0.001227 | 0.00429 | 0.000373 |
| FE-01 | -4.89603 | -4.67241 | 0.971664 | 0.264443 | 0.290084 | 0.905234 | 0.84129 | 0.991372 |
| FE-02 | -4.80684 | -4.75253 | 0.34643 | 0.066965 | 0.094682 | 0.714982 | 0.620571 | 0.911944 |
| FE-03 | -4.63054 | -4.61236 | 0.047404 | 0.699422 | 0.061999 | 0.242071 | 0.290952 | 0.800521 |
| FE-04 | -4.78595 | -4.74085 | 0.226973 | 0.14227 | 0.022821 | 0.475622 | 0.5922 | 0.783947 |
| FE-05 | -5.01063 | -4.72215 | 0.313643 | 0.011995 | 0.063712 | 0.85567 | 0.99051 | 0.962911 |
| FE-06 | -4.99874 | -4.72111 | 0.626031 | 0.00362 | 0.001123 | 0.251378 | 0.377595 | 0.924807 |
| FE-07 | -5.01593 | -4.82979 | 0.709514 | 0.033955 | 0.007602 | 0.250315 | 0.452032 | 0.977544 |
| FE-08 | -4.9402 | -4.73838 | 0.898789 | 0.001148 | 5.27E-05 | 0.20839 | 0.517116 | 0.998455 |
| FE-09 | -5.15495 | -5.04813 | 0.000675 | 0.324287 | 4.77E-07 | 0.005395 | 0.190669 | 0.985724 |
| FE-10 | -4.9352 | -4.73496 | 0.033187 | 0.012934 | 0.000169 | 0.000231 | 0.001955 | 0.835641 |
| FE-11 | -5.76508 | -4.81121 | 0.002572 | 0.246075 | 0.380592 | 0.053368 | 0.494964 | 0.463254 |
| FE-12 | -5.02832 | -4.82363 | 0.006106 | 0.110074 | 0.558088 | 0.878836 | 0.958792 | 0.905386 |
| FE-13 | -4.52167 | -4.7021 | 0.889392 | 0.000187 | 1.36E-05 | 0.008272 | 0.029892 | 0.956824 |
| FE-14 | -5.09587 | -4.80282 | 2.06E-05 | 0.014421 | 0.849536 | 0.738221 | 0.925655 | 0.438166 |
| FE-15 | -5.08278 | -4.85403 | 0.096426 | 1.61E-07 | 0.198504 | 0.369677 | 0.904156 | 0.998289 |

The distribution and metabolism properties of the selected compounds (FE-01 to FE-15) were analyzed and compared with Rofecoxib as the reference standard (Table 7). Rofecoxib exhibited high plasma protein binding (PPB = 93.45%), moderate volume of distribution (VD = −0.11), and significant blood–brain barrier permeability (BBB = 0.74), indicating efficient systemic distribution with central nervous system (CNS) accessibility. Additionally, Rofecoxib showed interaction with multiple CYP enzymes, particularly as a substrate of CYP1A2, CYP2C9, and CYP3A4, suggesting its metabolism is primarily enzyme-mediated.

Most of the tested compounds demonstrated high plasma protein binding (>80%), particularly FE-05, FE-06, FE-08, FE-12, FE-14, and FE-15 (>96%), indicating strong binding affinity to plasma proteins, which may prolong systemic circulation but reduce free drug concentration. In contrast, FE-03 and FE-11 showed low PPB values (~23–29%), suggesting a higher fraction of unbound drug available for pharmacological action.

The volume of distribution (VD) varied among compounds, where FE-12 (0.83) and FE-14 (0.59) exhibited higher VD values, indicating wider tissue distribution compared to Rofecoxib. Conversely, compounds such as FE-05, FE-06, and FE-11 showed negative VD values, suggesting limited tissue penetration. Regarding BBB permeability, FE-10 (0.97) showed the highest CNS penetration, exceeding that of Rofecoxib, followed by FE-08 (0.57) and FE-03 (0.45), indicating potential CNS activity. However, most compounds, including FE-01, FE-05, FE-06, FE-12, and FE-14, exhibited low BBB values, suggesting limited penetration into the brain, which may be advantageous in reducing CNS-related side effects. The fraction unbound (Fu) analysis indicated that compounds such as FE-03 and FE-11 had significantly higher unbound fractions (>70%), enhancing their bioactive availability. In contrast, highly lipophilic compounds (e.g., FE-05, FE-06, FE-12) showed low Fu values, indicating strong protein binding and reduced free drug concentration.

Metabolic profiling revealed diverse interactions with cytochrome P450 (CYP) enzymes. Compounds FE-05, FE-06, and FE-12 showed strong inhibitory effects on multiple CYP isoforms (CYP1A2, CYP2C19, CYP2C9, and CYP3A4), indicating a higher risk of drug–drug interactions. Similarly, FE-08 and FE-10 demonstrated significant CYP inhibition and substrate characteristics, suggesting complex metabolic behavior.

In contrast, FE-03 and FE-11 exhibited minimal CYP inhibition, indicating a lower risk of metabolic interactions. Notably, FE-15 demonstrated a balanced metabolic profile with moderate CYP inhibition and minimal substrate behavior across major isoforms, suggesting stable metabolism comparable to Rofecoxib. Overall, compared with Rofecoxib, compounds such as FE-02, FE-04, FE-13, and FE-15 exhibited favorable distribution and metabolic characteristics with balanced plasma protein binding,

moderate tissue distribution, controlled BBB permeability, and acceptable CYP interaction profiles. Among these, FE-15 stands out as a promising candidate due to its optimal balance between distribution and metabolism, reduced risk of drug–drug interactions, and similarity to the reference drug Rofecoxib.

**Table 7: Distribution and metabolism parameter of selected molecules**

| Compounds | Distribution | | | | Metabolism | | | | | | | | | |
|---|---|---|---|---|---|---|---|---|---|---|---|---|---|---|
| | | | | | CYP1A2 | | CYP2C19 | | CYP2C9 | | CYP2D6 | | CYP3A4 | |
| | PPB% | VD | BBB | Fu | Inhibitor | Substrate | Inhibitor | Substrate | Inhibitor | Substrate | Inhibitor | Substrate | Inhibitor | Substrate |
| Rofecoxib-NL | 93.45444 | -0.11274 | 0.746754 | 7.596543 | 0.113865 | 0.994333 | 0.047024 | 0.384455 | 0.01828 | 0.801853 | 6.52E-08 | 7.99E-07 | 1.88E-05 | 0.950402 |
| FE-01 | 95.13009 | 0.297543 | 0.002436 | 3.687188 | 0.884676 | 0.005608 | 0.820442 | 0.03017 | 0.082092 | 0.113102 | 0.012211 | 0.093058 | 0.020913 | 0.840268 |
| FE-02 | 86.32645 | -0.40505 | 0.066267 | 12.73905 | 0.989206 | 0.46211 | 0.300878 | 0.792644 | 0.103082 | 0.608688 | 0.09797 | 0.947399 | 0.892514 | 0.002264 |
| FE-03 | 23.21487 | -0.24099 | 0.455735 | 75.79157 | 0.000114 | 0.116644 | 0.000573 | 0.004567 | 2.40E-05 | 0.010498 | 1.31E-05 | 3.58E-06 | 0.068013 | 0.800068 |
| FE-04 | 84.24602 | 0.263718 | 0.156288 | 14.84473 | 0.829567 | 0.13949 | 0.262652 | 0.238959 | 0.12968 | 0.770187 | 0.099739 | 0.993369 | 0.909476 | 0.001636 |
| FE-05 | 99.33191 | -0.57211 | 8.83E-05 | 0.214343 | 0.999999 | 0.000295 | 0.999982 | 0.038681 | 0.934767 | 0.987306 | 0.082779 | 0.999997 | 0.985228 | 3.72E-07 |
| FE-06 | 98.12085 | -0.30672 | 0.005116 | 1.351312 | 0.999964 | 7.69E-06 | 0.999954 | 0.023234 | 0.93313 | 0.999979 | 0.019918 | 0.999495 | 0.999575 | 1.35E-07 |
| FE-07 | 84.06459 | -0.28325 | 0.074199 | 13.25603 | 4.90E-06 | 0.100387 | 0.038152 | 0.877276 | 0.000915 | 3.54E-06 | 0.002141 | 0.002362 | 0.006906 | 0.999997 |
| FE-08 | 96.87284 | 0.2294 | 0.571972 | 4.215422 | 0.000199 | 0.000151 | 0.77658 | 0.999979 | 0.985631 | 0.000636 | 0.395406 | 0.00111 | 0.098292 | 1 |
| FE-09 | 83.28198 | -0.16791 | 0.066315 | 15.48761 | 1.68E-06 | 1.82E-08 | 0.001562 | 0.003897 | 0.122845 | 9.22E-07 | 0.071877 | 0.009077 | 0.184067 | 0.989626 |

 © 2026 Author

| | | | | | | | | | | | | | | |
|---|---|---|---|---|---|---|---|---|---|---|---|---|---|---|
| FE-10 | 89.91205 | 0.070228 | 0.973039 | 10.37904 | 5.74E-09 | 0.010071 | 3.04E-05 | 0.998852 | 0.899025 | 0.916719 | 0.000734 | 0.019248 | 7.21E-05 | 0.999908 |
| FE-11 | 29.7781 | -0.52623 | 0.092296 | 74.90845 | 0.000115 | 0.0955 | 0.001409 | 0.118952 | 0.007833 | 0.034365 | 4.61E-05 | 0.000733 | 0.00227 | 0.11298 |
| FE-12 | 98.4501 | 0.836851 | 0.012967 | 1.623035 | 0.99489 | 0.012821 | 0.99395 | 0.054146 | 0.931453 | 0.953106 | 0.258867 | 0.998578 | 0.884083 | 0.000534 |
| FE-13 | 94.65341 | 0.384264 | 0.136011 | 6.228096 | 2.32E-05 | 0.998408 | 0.012102 | 1 | 0.000286 | 0.002561 | 0.00014 | 3.47E-05 | 0.872455 | 1 |
| FE-14 | 98.03125 | 0.592197 | 0.020998 | 1.671825 | 0.072816 | 8.23E-05 | 0.015061 | 0.061985 | 0.165551 | 0.99999 | 0.146891 | 0.732832 | 1.25E-05 | 5.50E-05 |
| FE-15 | 97.05022 | -0.15451 | 0.09206 | 2.433584 | 6.93E-05 | 1.12E-05 | 0.733609 | 9.75E-11 | 0.981409 | 0.000554 | 2.81E-07 | 6.51E-05 | 2.25E-06 | 5.51E-06 |

The excretion and toxicity profiles of the selected compounds (FE-01 to FE-15) were evaluated and compared with Rofecoxib as the reference standard (Table 8). Rofecoxib exhibited moderate plasma clearance (CL = 1.00) and half-life ($T_1/_2$ = 2.47 h), indicating sustained systemic exposure. However, it showed high probabilities of hepatotoxicity (H-HT = 0.93) and drug-induced liver injury (DILI = 0.99), highlighting known safety concerns associated with its clinical use.

In comparison, several compounds demonstrated improved excretion profiles. Compounds such as FE-02 (CL = 10.32), FE-04 (CL = 12.84), FE-07 (CL = 13.49), FE-08 (CL = 13.99), FE-09 (CL = 14.51), FE-10 (CL = 14.09), and FE-13 (CL = 11.41) showed significantly higher plasma clearance than Rofecoxib, suggesting rapid elimination and a lower risk of systemic accumulation. However, these compounds also exhibited shorter half-lives ($T_1/_2$ = 0.21–1.51 h), which may necessitate more frequent dosing. In contrast, FE-03 ($T_1/_2$ = 2.94 h) and FE-11 ($T_1/_2$ = 2.77 h) displayed longer half-lives comparable to Rofecoxib, indicating prolonged systemic retention.

Toxicity evaluation revealed that multiple compounds possess improved hepatic safety compared to Rofecoxib. Notably, FE-06 (DILI = 0.0003), FE-05 (0.03), FE-04 (0.12), and FE-01 (0.12) showed markedly reduced DILI probabilities, suggesting minimal risk of liver injury. Furthermore, hepatotoxicity values were also lower for several compounds, such as FE-06 (H-HT = 0.14) and FE-01 (0.24), compared to Rofecoxib. Mutagenicity assessment (Ames toxicity) indicated that FE-01 (0.10), FE-05 (0.03), FE-06 (0.18), FE-12 (0.08), and FE-14 (0.04) are likely non-mutagenic, whereas FE-03 (0.82) and FE-11 (0.79) showed higher mutagenic potential, which may limit their safety profile. Similarly, acute oral toxicity values suggested that most compounds (e.g., FE-05 = 0.06, FE-06 = 0.03) are less toxic than Rofecoxib (0.62), indicating improved safety margins.

The FDAMDD index, which reflects drug development potential, was highest for FE-10 (0.95), followed by FE-07 (0.62) and FE-08 (0.64), suggesting their suitability for further pharmaceutical development.

Skin sensitization analysis revealed high probabilities for many compounds, including FE-06 (0.99), FE-12 (0.96), and FE-15 (0.99), indicating potential dermatological risks. However, FE-10 (0.46) showed comparatively lower sensitization potential. Carcinogenicity evaluation demonstrated that FE-05 (0.20), FE-06 (0.05), FE-10 (0.36), and FE-14 (0.26) possess lower carcinogenic risk compared to Rofecoxib (0.93), indicating improved long-term safety. In contrast, FE-03 (0.87), FE-07 (0.88), and FE-13 (0.83) exhibited higher carcinogenic potential. Eye toxicity parameters showed that compounds such as FE-01 (0.94), FE-02 (0.99), and FE-04 (0.99) have high probabilities of eye corrosion and irritation, whereas FE-

10 (eye corrosion ≈ 0.00006) and FE-15 (≈ 0.000004) demonstrated negligible eye damage potential, indicating improved ocular safety.

Respiratory toxicity analysis indicated relatively high values for compounds like FE-14 (0.93) and FE-15 (0.97), while FE-03 (0.28) and FE-11 (0.05) showed lower respiratory toxicity risk. Overall, when compared with Rofecoxib, several compounds demonstrated enhanced safety and excretion profiles. In particular, FE-06 exhibited an excellent safety profile with very low DILI, mutagenicity, and carcinogenicity, while FE-10 showed strong drug development potential (high FDAMDD) with low eye toxicity. Importantly, FE-15 displayed a balanced profile with moderate clearance (CL = 3.67), acceptable half-life (1.34 h), reduced mutagenicity, negligible eye corrosion, and improved hepatic safety compared to Rofecoxib.

Thus, integrating excretion efficiency with toxicity parameters, FE-06, FE-10, and FE-15 emerge as the most promising candidates, offering safer pharmacokinetic and toxicological profiles than the reference drug Rofecoxib and warranting further experimental validation.

**Table 8: Excretion and Toxicity parameters of selected compounds**

| Compounds | Excretion | | Toxicity | | | | | | | | | |
|---|---|---|---|---|---|---|---|---|---|---|---|---|
| | CL-plasma | T1/2 | H-HT | DILI | Ames Toxicity | Rat Oral Acute Toxicity | FDAMDD | Skin Sensitization | Carcinogenicity | Eye Corrosion | Eye Irritation | Respiratory Toxicity |
| Rofecoxib-NL | 1.004093 | 2.473941 | 0.933564 | 0.998537 | 0.645177 | 0.625749 | 0.752919 | 0.983002 | 0.936911 | 0.000203 | 0.144448 | 0.04687 |
| FE-01 | 7.752417 | 0.493467 | 0.243233 | 0.12496 | 0.100422 | 0.403656 | 0.599786 | 0.624575 | 0.244733 | 0.946823 | 0.99461 | 0.768589 |
| FE-02 | 10.32476 | 1.517637 | 0.350741 | 0.165793 | 0.546391 | 0.365064 | 0.210007 | 0.929057 | 0.594417 | 0.990839 | 0.997473 | 0.746635 |
| FE-03 | 2.378667 | 2.949807 | 0.496423 | 0.690263 | 0.822678 | 0.262941 | 0.102621 | 0.850596 | 0.878551 | 0.644281 | 0.970911 | 0.282081 |
| FE-04 | 12.84532 | 1.318768 | 0.319301 | 0.121643 | 0.523285 | 0.500702 | 0.233956 | 0.965682 | 0.578103 | 0.99803 | 0.999112 | 0.612232 |
| FE-05 | 5.395384 | 0.437147 | 0.647367 | 0.030411 | 0.033088 | 0.062152 | 0.283709 | 0.996326 | 0.205236 | 0.875446 | 0.98076 | 0.880527 |
| FE-06 | 5.900761 | 0.243798 | 0.143158 | 0.000319 | 0.185467 | 0.039654 | 0.045761 | 0.999951 | 0.051452 | 0.999478 | 0.997832 | 0.687781 |

 © 2026 Author

| | | | | | | | | | | | | | |
|---|---|---|---|---|---|---|---|---|---|---|---|---|---|
| FE-07 | 13.49047 | 0.505655 | 0.701306 | 0.142992 | 0.281635 | 0.46995 | 0.62981 | 0.858337 | 0.887285 | 0.0002 | 0.066195 | 0.892466 | |
| FE-08 | 13.99287 | 0.572568 | 0.464818 | 0.017588 | 0.195402 | 0.262858 | 0.644655 | 0.709364 | 0.641227 | 0.231598 | 0.905975 | 0.803241 | |
| FE-09 | 14.51213 | 0.695179 | 0.556978 | 0.250527 | 0.216314 | 0.143735 | 0.6133 | 0.946994 | 0.874873 | 0.499903 | 0.956759 | 0.798543 | |
| FE-10 | 14.09679 | 0.499475 | 0.853836 | 0.109719 | 0.220476 | 0.489152 | 0.951205 | 0.46758 | 0.366524 | 6.69E-05 | 0.048765 | 0.843255 | |
| FE-11 | 2.187537 | 2.772336 | 0.304125 | 0.411401 | 0.796951 | 0.059916 | 0.025373 | 0.966495 | 0.242649 | 0.050136 | 0.891976 | 0.05976 | |
| FE-12 | 5.277782 | 0.520919 | 0.43337 | 0.147367 | 0.085875 | 0.147864 | 0.224237 | 0.965185 | 0.473063 | 0.990215 | 0.995925 | 0.884441 | |
| FE-13 | 11.41759 | 0.210759 | 0.611977 | 0.210093 | 0.163498 | 0.193499 | 0.255234 | 0.966408 | 0.838636 | 0.80516 | 0.940723 | 0.801598 | |
| FE-14 | 3.770445 | 0.932167 | 0.422959 | 0.187545 | 0.04709 | 0.124449 | 0.178303 | 0.908553 | 0.269677 | 0.98317 | 0.997497 | 0.932895 | |
| FE-15 | 3.674133 | 1.340398 | 0.585166 | 0.999999 | 0.12602 | 0.532644 | 0.313085 | 0.999965 | 0.482091 | 3.99E-06 | 0.235406 | 0.978512 | |

The environmental toxicity profile of the selected compounds (FE-01 to FE-15) was evaluated and compared with Rofecoxib as the reference standard (Table 9). Rofecoxib exhibited moderate bioaccumulation potential (BCF = 0.61) and baseline aquatic toxicity with IGC50 = 3.25, LC50FM = 4.05, and LC50DM = 4.50, indicating a balanced but notable environmental impact.

Among the tested compounds, FE-01, FE-07, FE-08, FE-09, FE-10, and FE-13 showed relatively higher bioaccumulation factors (BCF > 2), suggesting a greater tendency to accumulate in aquatic organisms compared to Rofecoxib. Particularly, FE-09 (BCF = 3.12) and FE-08 (BCF = 2.94) exhibited the highest bioaccumulation potential, which may raise environmental safety concerns despite their pharmacological promise. In contrast, compounds such as FE-03 (BCF = 0.22) and FE-11 (BCF = 0.24) demonstrated very low bioaccumulation, indicating a safer environmental profile in terms of accumulation. Similarly, FE-02, FE-14, and FE-15 showed BCF values comparable to Rofecoxib, suggesting moderate environmental persistence. The IGC50 values, which reflect toxicity toward aquatic protozoa, indicated that compounds like FE-08 (5.22), FE-10 (5.32), and FE-13 (5.15) are less toxic compared to Rofecoxib, as higher values

correspond to lower toxicity. Conversely, FE-11 (1.47) and FE-03 (2.64) exhibited lower IGC50 values, indicating higher toxicity toward microorganisms.

Similarly, fish toxicity (LC50FM) and daphnia toxicity (LC50DM) analyses revealed that compounds such as FE-08, FE-10, and FE-13 possess higher LC50 values (>6 for LC50FM in FE-10 and FE-08), indicating reduced toxicity and improved environmental safety relative to Rofecoxib. In contrast, FE-11 (LC50FM = 1.79) and FE-03 (3.11) showed lower LC50 values, suggesting higher aquatic toxicity. Interestingly, FE-05, FE-06, and FE-12 demonstrated moderate BCF values (~1.0–1.3) along with improved LC50DM values (>5.8), indicating a balanced environmental profile with reduced aquatic toxicity. Overall, compared with Rofecoxib, several compounds exhibited improved environmental safety, particularly FE-08, FE-10, and FE-13, which showed lower aquatic toxicity despite higher bioaccumulation potential. On the other hand, FE-03 and FE-11 may pose environmental risks due to their higher toxicity toward aquatic organisms. Importantly, FE-15 demonstrated a favorable environmental profile with moderate bioaccumulation (BCF = 0.85) and improved aquatic toxicity values (LC50FM = 4.93, LC50DM = 5.30) compared to Rofecoxib. ADMET Radar Most potent Compound with Native Ligand are displayed in Table 10.

**Table 9: Environmental toxicity profile of designed molecules**

| Compounds | BCF | IGC50 | LC50FM | LC50DM |
|---|---|---|---|---|
| Rofecoxib-NL | 0.611037 | 3.25081 | 4.054206 | 4.509732 |
| FE-01 | 2.775099 | 4.732297 | 5.774494 | 6.119455 |
| FE-02 | 0.890793 | 3.140793 | 3.457028 | 4.075699 |
| FE-03 | 0.225156 | 2.64435 | 3.117583 | 3.935305 |
| FE-04 | 1.352813 | 3.421544 | 3.870738 | 4.164013 |
| FE-05 | 1.074552 | 4.596312 | 4.29867 | 6.103879 |
| FE-06 | 1.369483 | 4.495504 | 4.339975 | 5.893758 |
| FE-07 | 2.420114 | 4.710728 | 5.494967 | 5.844705 |
| FE-08 | 2.946786 | 5.226481 | 6.388802 | 6.110887 |
| FE-09 | 3.125031 | 4.736946 | 5.429239 | 5.154125 |
| FE-10 | 2.783332 | 5.324623 | 6.585691 | 6.449205 |
| FE-11 | 0.241271 | 1.477416 | 1.795226 | 2.401345 |
| FE-12 | 1.066633 | 4.494909 | 4.29068 | 5.913338 |
| FE-13 | 2.840786 | 5.152084 | 6.142235 | 5.847967 |
| FE-14 | 0.810951 | 3.830714 | 1.540689 | 5.495133 |
| FE-15 | 0.851034 | 3.818738 | 4.939875 | 5.306319 |

**Table 10: ADMET Radar Most potent Compound with Native Ligand**

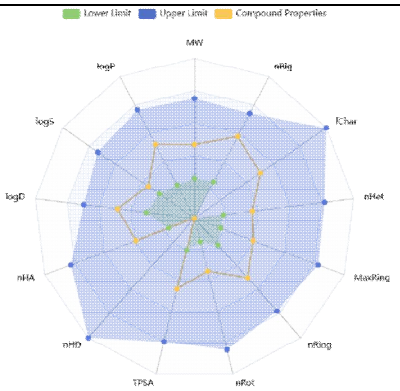


**Rofecoxib-NL**

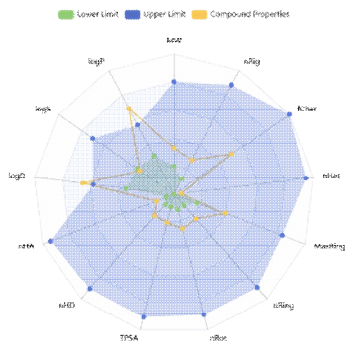


**FE-01**

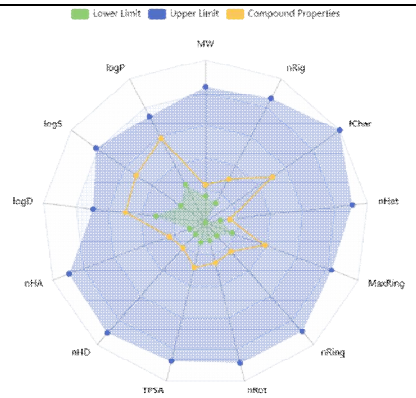


**FE-02**

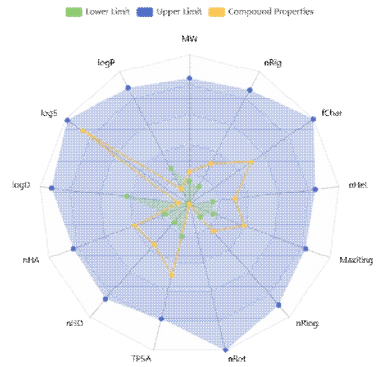


**FE-03**

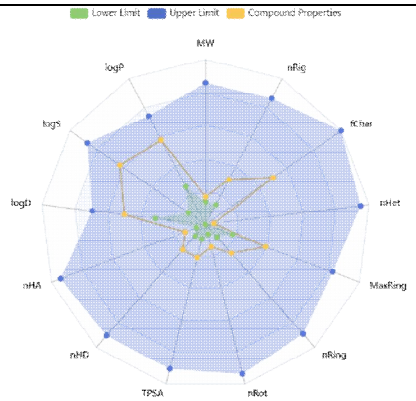


**FE-04**

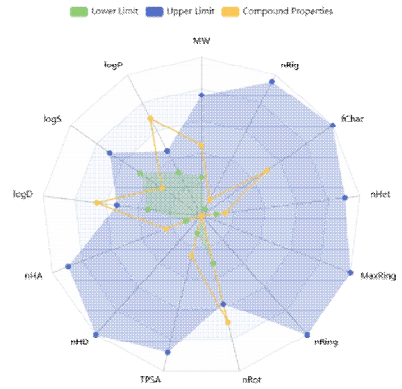


**FE-05**

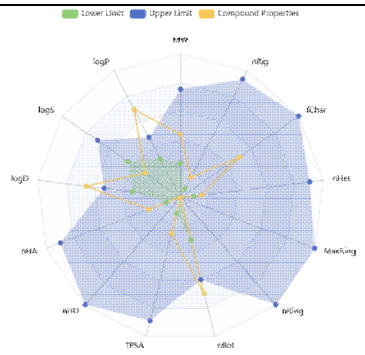


**FE-06**

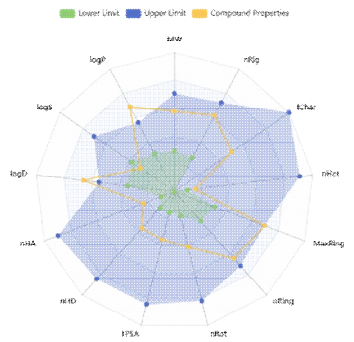


**FE-07**

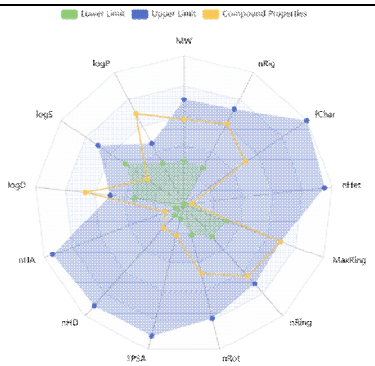


**FE-08**

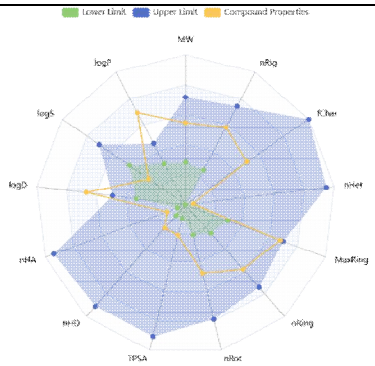


**FE-09**

 © 2026 Author

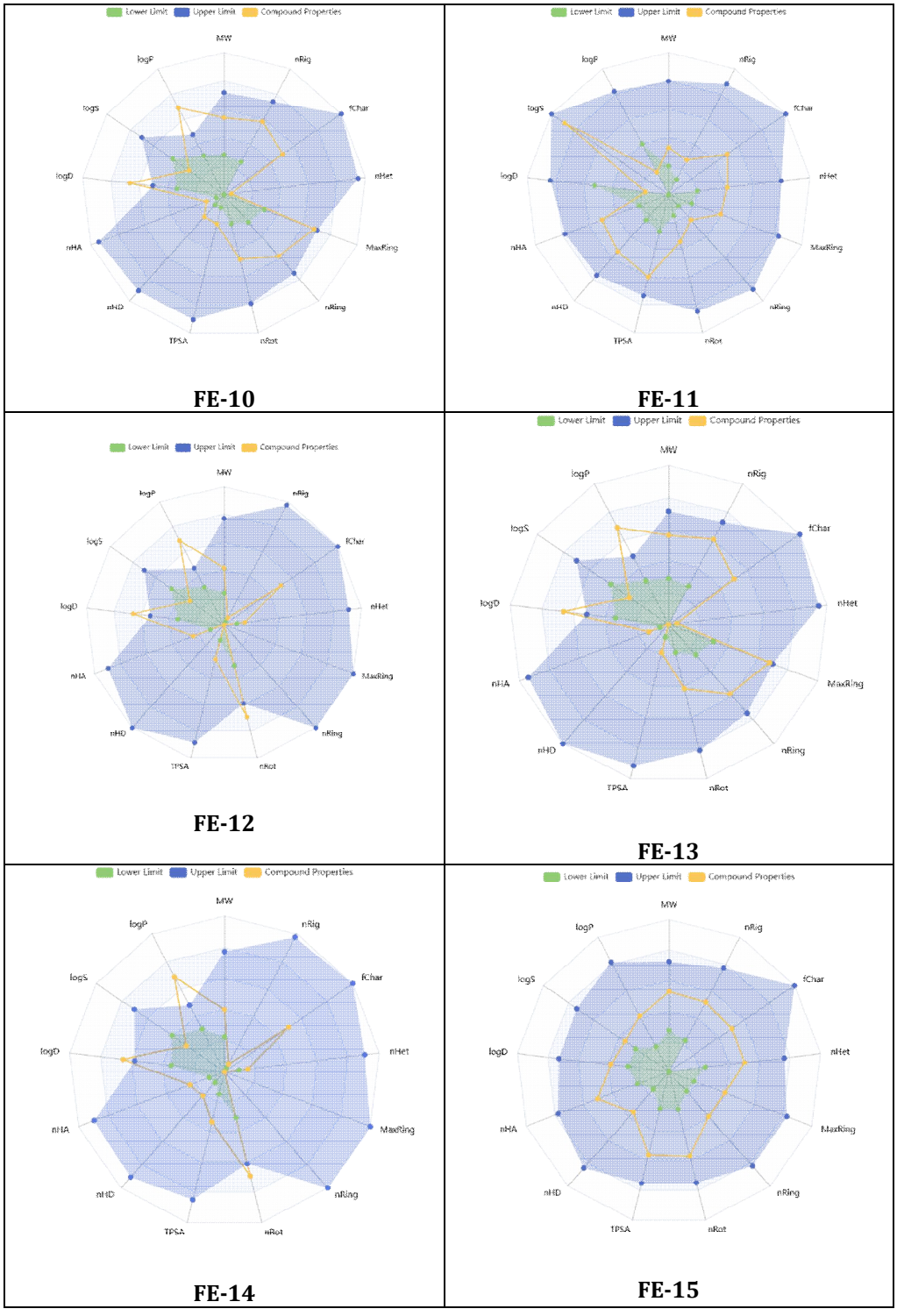


**FE-10** **FE-11**

**FE-12** **FE-13**

**FE-14** **FE-15**

## CONCLUSION

In conclusion, the present study successfully demonstrated the extraction, characterization, and pharmacological potential of *Feronia elephantum* using an integrated experimental and computational approach. The hydroalcoholic extraction method yielded a good percentage of extract with desirable physicochemical properties, confirming the quality, purity, and stability of the plant material. Preliminary phytochemical screening revealed the presence of diverse bioactive constituents, particularly lipids, phenolics, flavonoids, tannins, and steroids, which are known for their therapeutic significance. The extract was also found to be microbiologically safe, indicating proper handling and suitability for further applications. GC–MS analysis identified a wide range of phytoconstituents, including fatty acids, phenolic

compounds, sterols, and triterpenoids, with cyclolanostane derivatives as major components. Molecular docking studies revealed that several compounds, especially FE-09, FE-10, FE-13, and FE-15, exhibited strong binding affinity toward the COX-2 enzyme, comparable to or better than the standard drug Rofecoxib. Furthermore, ADMET and drug-likeness analysis highlighted FE-15, along with FE-02 and FE-04, as promising candidates with favorable pharmacokinetic and safety profiles. Overall, the study establishes *Feronia elephantum* as a potential source of bioactive compounds with anti-inflammatory activity and supports its further exploration for drug development and therapeutic applications.

**REFERENCES**


1. Akhlaq M, Alam, Mehboob MKAM. (2022). Potential of medicinal plants. Mediterr. J. Pharm. Pharm. Sci., 2, 13–21.
2. Dixit K, Chauhan B, Jain R. (2025). Anti-Inflammatory Potential of Medicinal Plants in the Management of Inflammatory Diseases: A Review of Mechanisms and Bioactive Compounds. J. Drug Deliv. Ther., 15, 330–40 https://doi.org/10.22270/jddt.v15i6.7203.
3. Manisha M, Babu R, Begam AM, Shakya Chahal K, Ashok Harale A. (2025). Medicinal Plants and Traditional Uses and Modern Applications. J. Neonatal Surg., 14, 162–75 https://doi.org/10.52783/jns.v14.2210.
4. Shah M, Parmar R, Patel K, Nagani A. (2024). Indole-based COX-2 inhibitors: A decade of advances in inflammation, cancer, and Alzheimer's therapy. Bioorg. Chem., 153, https://doi.org/ 10.1016/ j.bioorg.2024.107931.
5. Zaki M, Orban HA, Shahba MA, Moustafa RSI, Adel A, Fadel FI, Selim A, El-Bassyouni HT, Youness ER. (2025). The role of cyclooxygenase-2 (COX-2) and inflammatory markers in the progress of Alport syndrome in Egyptian children. BMC Pediatr., 25, https://doi.org/10.1186/s12887-025-05412-2.
6. Zhao L, Wang YF, Adamcakova-Dodd A, Thorne PS, Islam R, Liu KJ, Chen F, Luo J, Liu LZ. (2025). Nrf2/cyclooxygenase 2 signaling in Cr(VI)-induced carcinogenesis. Ecotoxicol. Environ. Saf., 291, https://doi.org/10.1016/j.ecoenv.2025.117800.
7. Sadiq SC, Joy MP, Aiswarya SU, Ajmani A, Keerthana CK, Rayginia TP, Isakov N, Anto RJ. (2024). Unlocking nature's pharmacy: an in-depth exploration of phytochemicals as potential sources of anti-cancer and anti-inflammatory molecules. Explor. Drug Sci., 2, 744–84 https://doi.org/10.37349/eds.2024.00073.
8. Sarwade PP, Nisha KB, Hari I, Tawale H, Ambika J, Thaiyalnayagi S, Yadav MK, (Sarwade) KNG, Geetha M. (2024). Phytochemical Analysis, Antioxidant Activity of Wild Medicinal Plants of Himalayan Range. J. Res. Appl. Sci. Biotechnol., 3, 131–46 https://doi.org/10.55544/jrasb.3.5.15.
9. Rabizadeh F, Mirian MS. (2024). The Classification of Medicinal Plants used in Traditional Persian Medicine for the Treatment of Liver Disease based on Phytochemical Properties. J. Med. Plants By-Products, 13, 257–84 https://doi.org/10.22034/jmpb.2023.363981.1623.
10. Oseni TE, Adejoh ME, Omowaye OS, Attah F, Peter J, Tennyson MA, Oladipe TT, Olubiyo CK, Oludare TT, Odiba JC, Ocean HO, Olopade TT. (2024). GC-MS Analysis, Qualitative and Quantitative Phytochemical Composition of *Boerhavia Diffusa* (Linn.) Leaf Extract Characterizing its Medicinal Use. Fudma J. Sci., 8, 144–51 https://doi.org/10.33003/fjs-2024-0806-2889.
11. Baba RT, Oluboyo BO, Egbebi AH, Aladodo M, Dangana ZA, Muhammad ZK, Sowole HB, Sani HU, Yakubu F. (2025). Investigation of the Phytochemical Constituents of *Euphorbia hirta* and *Senna alata* using Qualitative, Quantitative and Gas Chromatography–Mass Spectrometry (GC-MS) Analysis. Caliphate J. Sci. Technol., 7, 282–90 https://doi.org/10.4314/cajost.v7i2.11.
12. Alhudhaibi AM, Dahab M, Idriss H, Almoteri MF, Abdallah EM. (2025). Antibacterial properties of Solenostemma argel (Del.) Hayne against Salmonella strains from chicken meat: integrated GC–MS phytochemical profiling and molecular docking analysis. Front. Nutr., 12, https://doi.org/10.3389/fnut.2025.1694017.
13. Al-Gburi K, Naser NH, Jasamai M. (2026). Searching for newer histone deacetylase 6 inhibitors: Design, ADMET prediction, molecular docking, and molecular dynamics simulation of new Isatin hydrazones. Chem. Rev. Lett., 9, 98–112 https://doi.org/10.22034/crl.2025.517272.1583.
14. Siddiqui FA, Bakshi V. (2026). GC–MS-based analytical profiling of Lantana camara phytoconstituents and computational analysis for multi-target antidiabetic activity. J. Chem. Lett., 7, 1–24 https://doi.org /10.22034/ jchemlett.2026.571698.1375.
15. Shalbugau KW, Andema KA, Akinterinwa A, Yakubu J. (2025). Extraction And Chemical Profiling Of Luffa (*Luffa cylindrica* M. ROEM.) Seed Oil As a Potential Biodiesel Feedstock. Chem. Res. Technol., 2, 164–9.
16. Siddiqui Q, Shaikh YA. (2026). Hydroalcoholic Extraction of *Cissus quadrangularis* and In Vitro Evaluation of Antifungal Properties. J. PharmTechNova, 01, 3–10 https://doi.org/10.66220/vyc7rc95.
17. Eze V, Japhet T. (2025) . Quality Assessment of Groundwater Samples in Wukari Local Government Area , Taraba State. J. Chem. Technol., 1, 134–41 https://doi.org/10.22034/jchemtech.2025.539764.1024.
18. Ibrahim OM, Adeogo OE, Momoh IS, Afariogun SM, Ojelabi AO, Awonubi CO, Muhammed ME, Abdullahi AA. (2026). Phytochemicals Analysis and Antioxidant Potential of *Solanum erianthum* Leaf Extract in Mitigating $CCl_4$ -Induced Hepatic Damage. Med. Med. Chem., 3, 5–14.
19. Shaikh JR, Patil M. (2020). Qualitative tests for preliminary phytochemical screening: An overview. Int. J. Chem. Stud., 8, 603–8 https://doi.org/10.22271/chemi.2020.v8.i2i.8834.
20. Sheel DR, Nisha K, Kumar PJ. (2014). Preliminary Phytochemical Screening of Methanolic Extract Of *Clerodendron infortunatum.* IOSR J. Appl. Chem., 7, 10–3 https://doi.org/10.9790/5736-07121013.

21. Wang Z, Li H, Huang W, Duan S, Yan Y, Zeng Z, Fang Z, Li C, Hu B, Wu W, Lan X, Liu Y. (2024). Landscapes of the main components, metabolic and microbial signatures, and their correlations during pile-fermentation of Tibetan tea. Food Chem., 430, https://doi.org/10.1016/j.foodchem.2023.136932.
22. Zhuang X, Wang D, Jiang C, Wang X, Yang D, Zhang W, Xu S, Wang D, Zhuang X, Zhuang X, Jiang C, Wang X, Zhang W, Xu S, Wang D, Wang D. (2024). Achieving partial nitrification by sludge treatment using sulfide: Optimal conditions determination, long-term stability evaluation and microbial mechanism exploration. Bioresour. Technol., 408, https://doi.org/10.1016/j.biortech.2024.131207.
23. Khan SL, Bakshi V. (2026). Physicochemical characterization , GC – MS profiling , and computational evaluation of *Ailanthus excelsa* hydroalcoholic extract against mutant EGFR. Chem. Rev. Lett., 9, 358–76 https://doi.org /10.22034/crl.2026.571902.1771.
24. Siddiqui FS. (2026). Computational Assessment of Secondary Metabolites as Potential Inhibitors of Methylenetetrahydrofolate Dehydrogenase-2 ( MTHFD2 ). J. Phytopharm. Adv. Chem., 2, 3–17 https://doi.org /10.66220/wwze8340.
25. Roy D, Roy D. (2026). Drug repurposing of some US FDA-approved drugs using Binding strength Studies for the Treatment of Methicillin- resistant Staphylococcus aureus Infection. J. Phytopharm. Adv. Chem., 01, 30–44 https://doi.org/10.66220/ecsrwe33.
26. Pardaev J, Sadikova U. (2026). Computational Study of Alkaloids Targeting O-GlcNAc Transferase as Antidiabetic Agents. J. Phytopharm. Adv. Chem., 01, 18–29 https://doi.org/10.66220/qpba0t94.
27. Gandla K, Islam F, Zehravi M, Karunakaran A, Sharma I, Haque MA, Kumar S, Pratyush K, Dhawale SA, Nainu F, Khan SL, Islam MR, Al-Mugren KS, Siddiqui FA, Emran T Bin, Khandaker MU. (2023). Natural polymers as potential P-glycoprotein inhibitors: Pre-ADMET profile and computational analysis as a proof of concept to fight multidrug resistance in cancer. Heliyon, 9, https://doi.org/10.1016/j.heliyon.2023.e19454.
28. Mohammad BD, Baig MS, Bhandari N, Siddiqui FA, Khan SL, Ahmad Z, Khan FS, Tagde P, Jeandet P. (2022). Heterocyclic Compounds as Dipeptidyl Peptidase-IV Inhibitors with Special Emphasis on Oxadiazoles as Potent Anti-Diabetic Agents,. Molecules, 15;27(18):6001. doi: 10.3390/molecules27186001.

**Copyright: © 2026 Author**. This is an open access article distributed under the Creative Commons Attribution License, which permits unrestricted use, distribution, and reproduction in any medium, provided the original work is properly cited.